Parasitology Research (2020) 119:1523–1545
https://doi.org/10.1007/s00436-020-06628-0

GENETICS, EVOLUTION, AND PHYLOGENY - ORIGINAL PAPER

Multi-gene phylogeny of *Tetrahymena* refreshed with three new histophagous species invading freshwater planarians

Matej Rataj[1] · Peter Vďačný[1]

Received: 16 December 2019 / Accepted: 14 February 2020 / Published online: 9 March 2020

Abstract

Planarians represent an insufficiently explored group of aquatic invertebrates that might serve as hosts of histophagous ciliates belonging to the hymenostome genus *Tetrahymena*. During our extensive research on freshwater planarians, parasitic tetrahymenas were detected in two of the eight planarian species investigated, namely, in *Dugesia gonocephala* and *Girardia tigrina*. Using the 16S and 18S rRNA genes as well as the barcoding cytochrome oxidase subunit I, one ciliate species was identified as *T. scolopax* and three species were recognized as new forms: *T. acanthophora*, *T. dugesiae*, and *T. nigricans*. Thus, 25% of the examined planarian taxa are positive for *Tetrahymena* species and three of them represent new taxa, indicating a large undescribed ciliate diversity in freshwater planarians. According to phylogenetic analyses, histophagous tetrahymenas show a low phylogenetic host specificity. Although *T. acanthophora*, *T. dugesiae*, and *T. scolopax* clustered together within the "*borealis*" clade, the former species has been detected exclusively in *G. tigrina*, while the two latter species only in *D. gonocephala*. *Tetrahymena nigricans*, which has been isolated only from *G. tigrina*, was classified within the "*paravorax*" clade along with *T. glochidiophila* which feeds on glochidia. The present phylogenetic reconstruction of ancestral life strategies suggested that the last common ancestor of the family Tetrahymenidae was free-living, unlike the progenitor of the subclass Hymenostomatia which was very likely parasitic. Consequently, there were at least seven independent shifts back to parasitism/histophagy within *Tetrahymena*: one each in the "*paravorax*" and "*australis*" clades and at least five transfers back to parasitism in the "*borealis*" clade.

Keywords 16S and 18S rRNA genes · Ancestral life strategies · Ciliophora · Cytochrome oxidase subunit I · Diversification · Histophagy

Introduction

The hymenostome genus *Tetrahymena* Furgason, 1940 belongs together with *Paramecium* Müller, 1773 and *Oxytricha* Bory, 1824 among the best studied genera of the phylum Ciliophora Doflein, 1901 (Lynn 2008). The most explored *Tetrahymena* species is undoubtedly *T. thermophila* Nanney & McCoy, 1976, formerly classified in the *pyriformis* complex as *T. pyriformis* syngen 1 (Nanney and McCoy 1976). Its successful cultivation on sterile medium by Lwoff (1923) initiated a new chapter of research in the field of biochemistry and physiology of unicellular organisms. The easy cultivability of *T. thermophila* also contributed to several important discoveries, ranging from the existence of cell-cycle regulation mechanisms (Frankel 1999), through the activity of enzymes indispensable for DNA-matrix reproduction (Brownell et al. 1996; Greider and Blackburn 1985) to even a more significant finding from the medical perspective, the presence of tandem repeats of hexanucleotide units protecting chromosome ends (Blackburn and Gall 1978; Yao and Yao 1981; Yao et al. 1981).

The common morphological feature of this genus, from which its name also originated, is the structure of the oral

Handling Editor: Julia Walochnik

Electronic supplementary material The online version of this article (https://doi.org/10.1007/s00436-020-06628-0) contains supplementary material, which is available to authorized users.

✉ Matej Rataj
rataj2@uniba.sk

Peter Vďačný
peter.vdacny@uniba.sk

[1] Department of Zoology, Faculty of Natural Sciences, Comenius University in Bratislava, 842 15 Bratislava, Slovakia

ciliature. *Tetrahymena* possesses three oral polykinetids on the left and a single paroral membrane on the right of the oral cavity (Furgason 1940). Although this structure remains practically the same among different species, the size of the oral apparatus varies considerably, depending on the feeding strategy and life style.

Corliss (1969, 1970) provided first insights into the intrageneric taxonomy of *Tetrahymena* based on the following categories of characters: ciliature and cortex, life cycle, ecology, and physiologic as well as biochemical properties. As a result, Corliss (1970) proposed dividing tetrahymenas into three groups: (1) the *pyriformis* complex, containing bacteria-feeding microphagous ciliates with tendencies to become parasites; (2) the *rostrata* complex, gathering facultative histophagous and/or parasitic species often dividing inside of a cyst; and (3) the *patula* complex of non-parasitic, weakly histophagous but occasionally cannibalistic macrostome forms. However, these three complexes very likely do not reflect the evolutionary history of the genus, since they do not form distinct clusters in phylogenetic trees (Chantangsi et al. 2007; Doerder 2019; Lynn and Doerder 2012; Lynn et al. 2018; Quintela-Alonso et al. 2013; Pitsch et al. 2017; Rataj and Vďačný 2019; Strüder-Kypke et al. 2001; Zahid et al. 2014). On the other hand, the analysis of the D2 domain of the 23S rRNA gene (now designated as 28S rRNA gene) by Nanney et al. (1998) has suggested a parallel evolutionary origin of macrostomy and histophagy within the genus *Tetrahymena*, thus supporting Corliss' (1972) tentative evolutionary scenario. Likewise, the 18S rRNA gene has indicated that histophagy evolved among tetrahymenas several times convergently (Rataj and Vďačný 2019; Strüder-Kypke et al. 2001). This ribosomal gene has also suggested division of the genus *Tetrahymena* into two fundamental lineages—one leading to the *borealis* group and the second gathering species of the *australis* group (Jerome et al. 1996; Strüder-Kypke et al. 2001). In spite of a small portion of today known species involved in the early analyses, this image remained almost unchanged when further species have been added in 18S rRNA gene phylogenies. However, a slightly different branching pattern has been offered by the mitochondrial gene coding for cytochrome c oxidase subunit 1 (COI), placing several taxa outside the *australis*/*borealis* dichotomy (Kher et al. 2011; Lynn et al. 2018; Quintela-Alonso et al. 2013).

Until 2018, more than 40 species have been recognized in *Tetrahymena* (Lynn et al. 2018). An actual breakthrough is represented by the study of Doerder (2019), which introduced 37 new names for molecularly unique species, considering genetic distances in the 18S rDNA and COI sequences. Still, it is hard to determine the overall species richness within the genus *Tetrahymena* due to the uncovered hidden diversity of cryptic species or even lost isolates (Doerder 2019), not to mention the need for examination of all sorts of habitats or potential host organisms. Indeed, invertebrates represent an insufficiently explored habitat of parasitic and potentially new tetrahymenas, as indicated in our previous study (Rataj and Vďačný 2019). Although *Tetrahymena* infections of invertebrates have been only seldomly studied, it has been recognized that multiple *Tetrahymena* species can invade a broad variety of invertebrates. For instance, black flies can be parasitized by *T. dimorpha* Batson, 1983 (Batson 1983) or *T. rotunda* Lynn et al., 1981 (Lynn et al. 1981), alderflies by *T. sialidos* Batson, 1985 (Batson 1985), mosquitoes by *T. empidokyrea* Jerome et al., 1996 (Jerome et al. 1996), midges by *T. chironomi* Corliss, 1960 (Corliss 1960), slugs by *T. limacis* (Warren 1932) Kozloff, 1946 (Kozloff 1946) or *T. rostrata* (Kahl 1926) Corliss, 1952 (Brooks 1968), glochidia of freshwater mussels by *T. glochidiophila* Lynn et al., 2018 (Lynn et al. 2018), and freshwater planarians by *T. pyriformis* (Ehrenberg 1830) Lwoff, 1947 and *T. corlissi* Thompson, 1955 (Wright 1981) as well as by some other so far undescribed species (Rataj and Vďačný 2019).

In the present paper, we focused on the prevalence of tetrahymenas in eight freshwater planarian species. Associations of ciliates with planarians are an interesting emerging but still very insufficiently explored topic (Rataj and Vďačný 2018, 2019). Our extensive sampling yielded three new morphologically distinguishable histophagous *Tetrahymena* species, inhabiting the gut and mesenchyme tissues of freshwater planarians. We were also successful in amplifying three molecular markers (the nuclear 18S rDNA and the mitochondrial 16S rDNA and COI) of these parasitic tetrahymenas, which corroborated their distinctness and enabled us to study the evolution of histophagy in hymenostomes from the phylogenetic perspective. And, finally, the three *Tetrahymena* species parasitizing planarians are formally described here as new taxa.

Material and methods

Material collection and processing

Collection, identification, storage, and consecutive dissection of host organisms were carried out as described in our previous publications (Rataj and Vďačný 2018, 2019). During the course of this study, samples were obtained together from 27 collection sites between October 2016 and May 2019. These sites were represented by the coastal zones of lakes, slowly running streams as well as by the shallow sections of bigger rivers in Slovakia. Their characterization with GPS coordinates and corresponding planarian species is summarized in Table 1.

Altogether, 784 planarians were inspected for the presence of tetrahymenas. Representative specimens of each planarian species are shown in Supplementary Fig. S1. Living *Tetrahymena* individuals were isolated from the mesenchyme and dissected gastrointestinal tissues of host organisms using

Table 1 Characterization of collection sites of freshwater planarians and occurrence *Tetrahymena* species

Collection date (m/d/y)	Site code	Collection site	Water body	GPS coordinates	Host species	Ta	Td	Tn	Ts
10/01/2016	1	Municipal forest park, Kačínska dolina valley, Železná studnička, Bratislava, Malé Karpaty Mts. (Little Carpathians)	Malá Vydrica stream	48° 12′ 05.9″ N, 17° 04′ 34.7″ E	*Dugesia gonocephala*	–	+	–	–
10/01/2016	2	Municipal forest park, Drieňovská lúka meadow, Železná studnička, Bratislava, Malé Karpaty Mts. (Little Carpathians)	Drieňovská dráha stream	48° 11′ 39.3″ N, 17° 05′ 50.8″ E	*Dugesia gonocephala*	–	–	–	–
10/08/2016	3	Spruce forest, Olešná Potôčky, district of the village of Olešná, Turzovská vrchovina highlands	Olešňanský potok stream	49° 26′ 08.7″ N, 18° 38′ 39.6″ E	*Dugesia gonocephala*	–	+	–	–
10/08/2016	4	Inundation area in the vicinity of the village of Milošová, Turzovská vrchovina highlands	Milošovanský potok stream	49° 28′ 17.1″ N, 18° 45′ 18.4″ E	*Dugesia gonocephala*	–	+	–	+
10/22/2016	5	Drieňovecká mokraď swamp, Slovenský kras (Slovak Karst) National Park, Slovenské Rudohorie (Slovak Ore Mts.)	Bercz spring area	48° 36′ 54.7″ N, 20° 54′ 54.8″ E	*Polycelis felina*	–	–	–	–
10/29/2016	6	Urban oak-hornbeam forest, Pekná cesta, Bratislava, Malé Karpaty Mts. (Little Carpathians)	Vajspeterský potok stream	48° 12′ 47.3″ N, 17° 07′ 21.1″ E	*Dugesia gonocephala*	–	+	–	–
10/29/2016	7	Urban oak-hornbeam forest, Knižková dolina valley, Bratislava, Malé Karpaty Mts. (Little Carpathians)	Banský potok stream	48° 13′ 08.8″ N, 17° 07′ 58.8″ E	*Dugesia gonocephala*	–	–	–	–
11/05/2016	8	Urban oak-hornbeam forest, Medené Hámre, district of the village of Borinka, Malé Karpaty Mts. (Little Carpathians)	Forest rainwater pool	48° 16′ 03.1″ N, 17° 07′ 16.0″ E	*Dugesia gonocephala*	–	–	–	–
11/05/2016	9	Municipal park, Tovarníky, district of the town of Topoľčany, Nitrianska pahorkatina highlands	Tovarníky fishpond	48° 34′ 07.9″ N, 18° 08′ 45.9″ E	*Girardia tigrina*	–	–	+	–
11/12/2016	10	Regulated stream in the town of Rajecké Teplice, Rajecká kotlina basin, Malá Fatra Mts.	Bystrička stream	49° 07′ 21.4″ N, 18° 41′ 16.9″ E	*Dugesia gonocephala*	–	–	–	–
11/19/2016	11	Pine-spruce forest, district of the village of Čadečka, Kysucké Beskydy Mts.	Čadečanský potok stream	49° 27′ 54.9″ N, 18° 49′ 02.9″ E	*Dugesia gonocephala*	–	–	–	–
11/16/2018	12	Urban oak-hornbeam forest, Pekná cesta, Bratislava, Malé Karpaty Mts. (Little Carpathians)	Vajspeterský rybník fishpond	48° 12′ 20.8″ N, 17° 07′ 42.4″ E	*Girardia tigrina*	–	–	–	–
11/25/2018	13	Recreation area in the village of Veľký Biel, Podunajská rovina plain	Veľkobielske jazero lake	48° 12′ 26.4″ N, 17° 21′ 28.3″ E	*Girardia tigrina*	+	–	+	–
12/02/2018	14	Recreation area in the village of Rovinka, Podunajská rovina plain	Rovinské štrkovisko lake	48° 05′ 57.2″ N, 17° 13′ 34.4″ E	*Girardia tigrina*	–	–	–	–
12/06/2018	15		Kalné jazero fishpond	48° 11′ 36.7″ N, 17° 10′ 39.2″ E	*Girardia tigrina*	+	–	–	–

Table 1 (continued)

Collection date (m/d/y)	Site code	Collection site	Water body	GPS coordinates	Host species	Ta	Td	Tn	Ts
		Eutrophic fishpond, Východné, Bratislava, Podunajská rovina plain							
12/06/2018	16	Municipal recreation area, Bratislava, Podunajská rovina plain	Zlaté Piesky lake	48° 11′ 04.0″ N, 17° 11′ 11.0″ E	*Girardia tigrina*	+	–	–	–
12/08/2018	17	Alluvial forest, Rusovce, Bratislava, Podunajská rovina plain	Rusovecké jazero lake	48° 03′ 45.9″ N, 17° 09′ 16.5″ E	*Girardia tigrina*	–	–	–	–
12/16/2018	18	Municipal recreation area, district of the village of Dunajská Lužná, Podunajská rovina plain	Malé Košariská lake	48° 05′ 50.5″ N, 17° 16′ 44.0″ E	*Girardia tigrina*	–	–	–	–
02/09/2019	19	Artificial lake, Vajnory, Bratislava, Podunajská rovina plain	Vajnorské jazero lake	48° 11′ 35.3″ N, 17° 12′ 34.9″ E	*Dendrocoelum lacteum*/*Schmidtea lugubris*	–/–	–/–	–/–	–/–
02/17/2019	20	Residential area Fončorda, Banská Bystrica, Zvolenská kotlina basin	Unnamed stream	48° 43′ 21.4″ N, 19° 06′ 58.3″ E	*Dugesia gonocephala*	–	–	–	–
03/07/2019	21	Shallow river section near the village of Stankovany, Veľká Fatra Mts.	Váh river	49° 08′ 26.3″ N, 19° 10′ 14.6″ E	*Dugesia gonocephala*	–	–	–	–
03/07/2019	22	Shallow river section near the village of Bystrá, Veľká Fatra Mts.	Váh river	49° 05′ 04.8″ N, 19° 17′ 07.7″ E	*Dugesia gonocephala*	–	–	–	–
03/07/2019	23	Pine-spruce forest, Hrabovská dolina valley, Veľká Fatra Mts.	Hrabovský potok stream	49° 04′ 15.0″ N, 19° 16′ 22.2″ E	*Polycelis felina*	–	–	–	–
03/07/2019	24	Pine-spruce forest, Čutkovská dolina valley, Veľká Fatra Mts.	Čutkovský potok stream	49° 04′ 53.7″ N, 19° 15′ 19.6″ E	*Polycelis felina*	–	–	–	–
03/23/2019	25	Urban oak-hornbeam forest, district of the village of Svätý Jur, Malé Karpaty Mts. (Little Carpathians)	Jurské jazierko pond	48° 15′ 28.0″ N, 17° 09′ 14.6″ E	*Schmidtea polychroa*/*Polycelis nigra*	–/–	–/–	–/–	–/–
04/06/2019	26	Artificial pond, Východné, Bratislava, Podunajská rovina plain	Unnamed pond	48° 12′ 08.7″ N, 17° 09′ 51.9″ E	*Girardia tigrina*	–	–	–	–
05/09/2019	27	Bielovodská dolina valley, Vysoké Tatry Mts. (High Tatra)	Biela voda river	49° 14′ 29.9″ N, 20° 06′ 04.7″ E	*Crenobia alpina*	–	–	–	–

Presence is designated by plus (+), absence by dash (−)

Ta, *T. acanthophora*; Td, *T. dugesiae*; Tn, *T. nigricans*; Ts, *T. scolopax*

an adjusted Pasteur micropipette (Foissner 2014). They were consequently washed through several drops of physiological saline solution (0.6% NaCl). Some sufficiently washed ciliates with no visible surrounding tissue particles were then put into the lysis buffer for later DNA extraction. Individual samples contained one, usually two, and rarely up to five *Tetrahymena* cells. Sequencing chromatograms of samples containing from one to five cells gave no evidence of multiple peaks, documenting that a single *Tetrahymena* species was analyzed each time. Other successfully isolated cells were subjected to a thorough morphological examination under an optical microscope Zeiss Axio Imager 2 equipped with differential interference contrast optics. Cell shape, ciliary pattern, locomotory behavior, contractile vacuole cycle together with other observable characteristics were captured on microphotographs and videos by a Canon EOS 70D camera with a format size of 1920 × 1080 pixels and a rate of 25 frames per second. All size measurements were conducted in ImageJ ver. 1.49. Illustrations consist of free-hand drawings and sketches made in Inkscape ver. 0.92.4, all based on microphotographs.

ZooBank registration number of the present work (Recommendation 8A of the International Commission on Zoological Nomenclature 2012) is urn:lsid:zoobank.org:pub:900AC676-1F58-49E6-95D2-7BC98E64C4FE.

Molecular methods

Thoroughly washed cells of *Tetrahymena* spp. intended for DNA extraction were lysed in 180 μl of cell lysis buffer (Promega, Fitchburg, Wisconsin, USA) and stored in a refrigerator at 8 °C until processed. DNA extraction followed the protocol of the Relia Prep™ Blood gDNA Miniprep System (Promega). Amplification of the nuclear 18S rRNA gene was performed using universal forward and reverse eukaryotic primers EukA (5′-AAC CTG GTT GAT CCT GCC AGT-3′) and EukB (5′-TGA TCC TTC TGC AGG TTC AC-3′) (Medlin et al. 1988). The respective thermo cycler program consisted of three stages: (i) initial hot start incubation of 15 min at 95 °C; (ii) 30 identical amplification cycles, each composed of 45 s denaturation at 95 °C, 1 min primer annealing at 55 °C, and 2.5 min extension at 72 °C; and (iii) final extension of 10 min at 72 °C (Vďačný et al. 2011). In the case of the mitochondrial 16S rRNA gene, amplification was carried out with 16S-mtSSU-F (5′-TGT GCC AGC AGC CGC GGT AA-3′) and 16S-mtSSU-R (5′-CCC MTA CCR GTA CCT TGT GT-3′) (van Hoek et al. 2000) primers. The respective PCR reaction was composed of four stages: (i) initial hot start incubation of 3 min at 94 °C; (ii) 5 amplification cycles (denaturing at 94 °C for 30 s, annealing at 50 °C for 1 min, and extension at 68 °C for 75 s); (iii) 30 amplification cycles (denaturing at 94 °C for 30 s, annealing at 60 °C for 1 min, and extension at 68 °C for 75 s); and (iv) final extension at 68 °C for 10 min (Lynn and Strüder-Kypke 2006). Finally, the mitochondrial COI gene was amplified using COI-FW-mod (5′-ATG TGA GTT GAT TTT ATA GA-3′) (Chantangsi et al. 2007) and COI-689-RW (5′-CTC TTC TAT GTC TTA AAC CAG GCA-3′) (Doerder 2014) primers and a slight modification of the previous PCR program. Thus, the primer annealing temperature of the stages (ii) and (iii) was lowered from 50 to 45 °C and from 60 to 55 °C, respectively, and the number of cycles in the stage (iii) was increased from 30 to 35. Quality check of the amplified DNA was constantly performed by agarose gel electrophoresis. PCR products of high quality were purified using the NucleoSpin Gel and PCR clean-up Kit (Macherey-Nagel) and consequently sequenced on an ABI 3730 automatic sequencer (Macrogen) with primers used for DNA amplification. The newly obtained sequences were inspected for quality in Chromas ver. 2.33 (Technelysium Pty Ltd) and the noise-free sequence fragments with strong signal were trimmed and assembled into contigs using BioEdit ver. 7.2.5 (Hall 1999).

Phylogenetic methods

Datasets and alignment procedures

Four sets of alignments were assembled to assess the phylogenetic position of three new *Tetrahymena* species. The first dataset contained concatenated sequences of the nuclear 18S rRNA gene and the mitochondrial COI gene, coming from 98 *Tetrahymena* spp. and some related hymenostomes (Supplementary Table S1). All *Tetrahymena* strains having sequences of both molecular markers have been selected for this dataset (Chantangsi et al. 2007; Doerder 2014, 2019; MacColl et al. 2015). The second dataset consisted of two concatenated mitochondrial markers, the 16S rRNA gene and COI, belonging to 22 *Tetrahymena* taxa (Supplementary Table S2). This dataset was distinctly smaller, since only comparatively few strains have available sequences from both markers. Because there were much more *Tetrahymena* GenBank entries with only one molecular marker available, two further alignments were constructed to cover the known diversity of the genus *Tetrahymena*. One contained 106 COI sequences and the second one consisted of 84 sequences coding for the 16S rRNA molecule. Sampling in these two alignments followed mainly Doerder (2019).

All sequences, except for those obtained in the present study, were downloaded from GenBank (https://www.ncbi.nlm.nih.gov/genbank/). The 16S rRNA gene and COI sequences used in the second alignment were extracted from the whole mitochondrial genomes (Brunk et al. 2003; Burger et al. 2000; Edqvist et al. 2000; Moradian et al. 2007). Ribosomal RNA genes were aligned with the ClustalW algorithm as implemented in BioEdit. The protein-coding COI gene sequences were aligned based on the predicted amino acid sequences with MEGA-X (Kumar et al. 2018), using

the protozoan mitochondrial genetic code and the Muscle codon algorithm. No masking strategy was employed, since all columns were aligned unambiguously.

Tree-building methods

The evolutionary history of tetrahymenas was reconstructed in the maximum likelihood (ML) and Bayesian frameworks. Both analyses were run on the CIPRES portal ver. 3.1 (http://www.phylo.org/) (Miller et al. 2010). ML trees were calculated with IQ-TREE on XSEDE ver. 1.6.10 (Nguyen et al. 2015). The model tester implemented in the IQ-TREE package was used to select the best model for each gene, according to the Bayesian Information Criterion. To assess the reliability of the branching pattern of the ML trees, 1000 non-parametric bootstrap replicates were conducted. Bayesian inferences (BI) were carried out in the program MrBayes on XSEDE ver. 3.2.7 (Ronquist et al. 2012) under the best evolutionary models selected for each molecular marker separately in jModelTest ver. 2.1.10 on the basis of the Akaike Information Criterion (Darriba et al. 2012). The settings of the MCMC analysis were as follows: (i) four simultaneously running chains, one cold and three heated; (ii) five million generations and a sampling frequency of one hundred; and (iii) the burn-in fraction of 25%.

Reconstruction of ancestral character states

Reconstruction of ancestral life strategies of the subclass Hymenostomatia Delage and Herouard, 1896 was conducted in SIMMAP ver. 1.5.2 (Bollback 2006). Two character states were considered: a parasitic (histophagic) and a free-living life style. Data were mostly obtained from Lynn et al. (2018), Doerder (2019), and references cited therein. Priors for ancestral state analysis were estimated from the 50% majority-rule Bayesian consensus tree inferred from the first dataset, using an MCMC analysis implemented in SIMMAP. The R script provided with the SIMMAP package was used to find the best fitting distribution for samples from the posterior distributions of the MCMC analyses. Priors of the ancestral states reconstruction analysis were (i) $\alpha = 1.00$ and $k = 31$ for the beta distribution of state frequencies; (ii) equal bias prior $1/k$ for the beta distribution; and (iii) $\alpha = 2.399$, $\beta = 0.036$, and $k = 60$ for the gamma distribution of the overall rate of character change. A set of 1000 trees was generated from the posterior distribution of the Bayesian analysis of the first concatenated alignment, using a custom Python script containing a random sampling function. The randomly selected post burn-in trees served to incorporate phylogenetic uncertainty. Ten samples were analyzed per each tree with 20 priors drawn from the prior distributions. Branch lengths were re-scaled that the overall length of trees is one. Results were plotted as pie charts and mapped onto the 50% majority-rule Bayesian consensus tree using the R script "PlotSimMap.R" (https://github.com/nylander/PlotSimMap).

Diversification analyses

The effect of life styles on diversification of tetrahymenas over their evolutionary history was assessed using the binary-state speciation and extinction (BiSSE) method (Maddison et al. 2007), as implemented in the program BayesRate ver. 1.3.41 (Silvestro et al. 2011). The BiSSE model has six free parameters: speciation (λ_0, λ_1) and extinction (μ_0, μ_1) rate for each character state as well as a transition rate of change between the two states (q_{01}, q_{10}). These six parameters were variously constrained to specify nested diversification models. Bayesian analyses were performed for each model over a sample of 1000 randomly selected trees from the posterior distribution of the Bayesian analysis of the first concatenated dataset. Trees were mid-point rooted and ultrametrized using a custom R script and the "force.ultrametric" function with the "extend" method, as implemented in the R-package phylotools (Revell 2012). MCMC simulations included 200 iterations of slice sampling per tree. The first 20 samples per tree were discarded as burn-in. Diffuse priors were set for the diversification-rate parameters, following Johnson et al. (2011). Finally, log marginal likelihoods were estimated for each model with the thermodynamic integration option. Nested models (M_0) were compared with the full model (M_1), using the Bayes factor test which is defined as the ratio between their marginal likelihoods. Thus, the log Bayes factor (BF) between pairs of models M_0 and M_1 can be calculated as $BF = 2(M_1 - M_0)$. According to Kass and Raftery (1995), $BF = 2$–6 is interpreted as positive evidence against M_0, $BF = 6$–10 as strong evidence, and $BF > 10$ as very strong evidence.

Since Bayes factor tests provided positive to very strong evidence against all nested models, posterior distributions of all diversification parameters (speciation and extinction rate for each character state and transition rates of change between the two states) were calculated under the full model. The MCMC simulations with exponential prior were conducted on the ultrametrized 50% majority-rule Bayesian consensus tree inferred from the first dataset, using the R-package diversitree (FitzJohn 2012). The step argument w for the MCMC sampler was determined by running a 100-step long chain. The range of observed samples was then used as a measure of the "step size" in a 10,000-step long MCMC chain. The 95% credibility intervals for marginal distributions of diversification parameters were calculated and plotted using the R "profiles.plot" function.

Results

Distribution and prevalence of *Tetrahymena* in planarians

Altogether eight freshwater planarian species, belonging to two ecological groups, were collected in the territory of Slovakia, Central Europe, and investigated for the presence of ciliates during the years 2016 and 2019. The first ecological group contained planarians sampled in a variety of running waters: 165 specimens of *Dugesia gonocephala* (Dugès, 1830) Girard, 1850; 169 individuals of *Polycelis felina* (Dalyell, 1814) Ehrenberg, 1831; and four exemplars of *Crenobia alpina* (Dana, 1766) Kenk, 1930. The second group included planarians from stagnant waters: 424 specimens of *Girardia tigrina* (Girard, 1850) Ball, 1974; eight individuals of *Dendrocoelum lacteum* (Müller, 1774) Ørsted, 1844; seven exemplars of *Schmidtea lugubris* (Schmidt, 1861) Ball, 1974; six specimens of *Schmidtea polychroa* (Schmidt, 1861) Ball, 1974; and a single individual of *Polycelis nigra* (Müller, 1774) Ehrenberg, 1831.

Three new histophagous species of the genus *Tetrahymena* were discovered after dissection of 784 planarian exemplars. However, only individuals of *D. gonocephala* and *G. tigrina*, the most abundant planarian species in each type of the aquatic environments, were found to be parasitized (Table 1). Interestingly, *D. gonocephala* was parasitized only by a single *Tetrahymena* species, described here as *T. dugesiae* sp. n. The cells of *T. dugesiae* were found only in 17 out of the 165 examined *D. gonocephala* individuals, which corresponds to a prevalence of approximately 10.3%. As concerns the two other *Tetrahymena* species, *T. acanthophora* sp. n., and *T. nigricans* sp. n., they were detected solely inside of *G. tigrina*. Simultaneous infections by both *Tetrahymena* species were noted only at a single collection site (Table 1). *Tetrahymena* infections in *G. tigrina* were rarer than in *D. gonocephala*. Specifically, *T. acanthophora* was detected in 14 out of the 424 examined *G. tigrina* individuals, which corresponds to a prevalence of ca. 3.3%. The prevalence of *T. nigricans* was even lower than 1%, since this ciliate appeared only in four planarians at two collection sites and always only a single cell per planarian was recorded. This makes *T. nigricans* the rarest among the three new tetrahymenas described in this paper. In addition to the three new *Tetrahymena* species, a single already described species, *T. scolopax* Doerder, 2019, was detected in *D. gonocephala* at one sampling site (Table 1). This species was identified based on the COI sequence (100% identity). The Slovak isolate of *T. scolopax* co-occurred with *T. dugesiae*.

No signs of pathological changes were detected in *G. tigrina* specimens infected by *T. acanthophora* and *T. nigricans*. The only indication of parasitism included the presence of planarian tissues in food vacuoles of both ciliate species. On the other hand, some *D. gonocephala* exemplars infected by *T. dugesiae* had open wounds. Possibly this *Tetrahymena* species enters planarians through wounds and then begins to feed on their mesenchyme. The numbers of *T. acanthophora* in *G. tigrina* ranged from one to about 50 cells (on average 11 cells, $n = 14$), while only a single cell of *T. nigricans* per host was detected each time ($n = 4$). The abundance of *T. dugesiae* per planaria varied from one to 15 cells (on average four cells, $n = 17$). All our attempts to cultivate the two former *Tetrahymena* species on the mesenchyme tissues failed, while one temporary culture of *T. dugesiae* was established in a Petri dish, using the *D. gonocephala* tissues.

Description of *Tetrahymena acanthophora* sp. n.

ZooBank registration number: urn:lsid:zoobank.org:act:30865328-6B2A-44FD-AD5F-918E31AB8B76.

Diagnosis: Size about 110 × 55 μm. Body elliptical, ovate or clavate with anterior end apiculate and posterior end broadly rounded. Macronucleus oval with a single large nucleolus. Contractile vacuole dorsal and subterminal. About 28 to 30 sigmoidal ciliary rows on each body side, no caudal cilia. Oral apparatus about 10 μm long.

Type locality: Veľkobielske jazero lake, recreation area in the village of Veľký Biel, Podunajská rovina plain (48° 12′ 26.4″ N, 17° 21′ 28.3″ E).

Type host: *Girardia tigrina* (Girard, 1850) Ball, 1974.

Type material: A DNA sample of holotype specimen has been deposited in Natural History Museum, Vajanského nábrežie 2, 810 06 Bratislava, Slovakia (ID Collection Code 1427132).

Gene sequences: The nuclear 18S rRNA gene sequence of holotype specimen has been deposited in GenBank (accession no. MN994469). The sequence is 1712 nucleotides long and has a GC content of 43.11%. The mitochondrial 16S rRNA gene sequence of holotype specimen has been deposited in GenBank (accession no. MN994474). The sequence is 996 nucleotides long and has a GC content of 29.92%. The COI gene sequence of holotype specimen has been deposited in GenBank (accession no. MN991314). The sequence is 946 nucleotides long and has a GC content of 25.58%.

Etymology: The specific epithet *acanthophora* is a composite of the stem of the Greek noun *ákantha* (ἄκανθα, thorn), the thematic vowel *·o-*, and the Latinized Greek adjective *phor·us*, *–a*, *–um* [m, f, n] (bearing), referring to the apiculate anterior pole of the body.

Description: The body size was approximately 83–133 × 32–73 μm ($n = 10$) in free-swimming individuals. The shape was elliptical, broadly to narrowly ovate or clavate but might have become fusiform after manipulation with a micropipette. The anterior body end was differentiated into a conspicuous

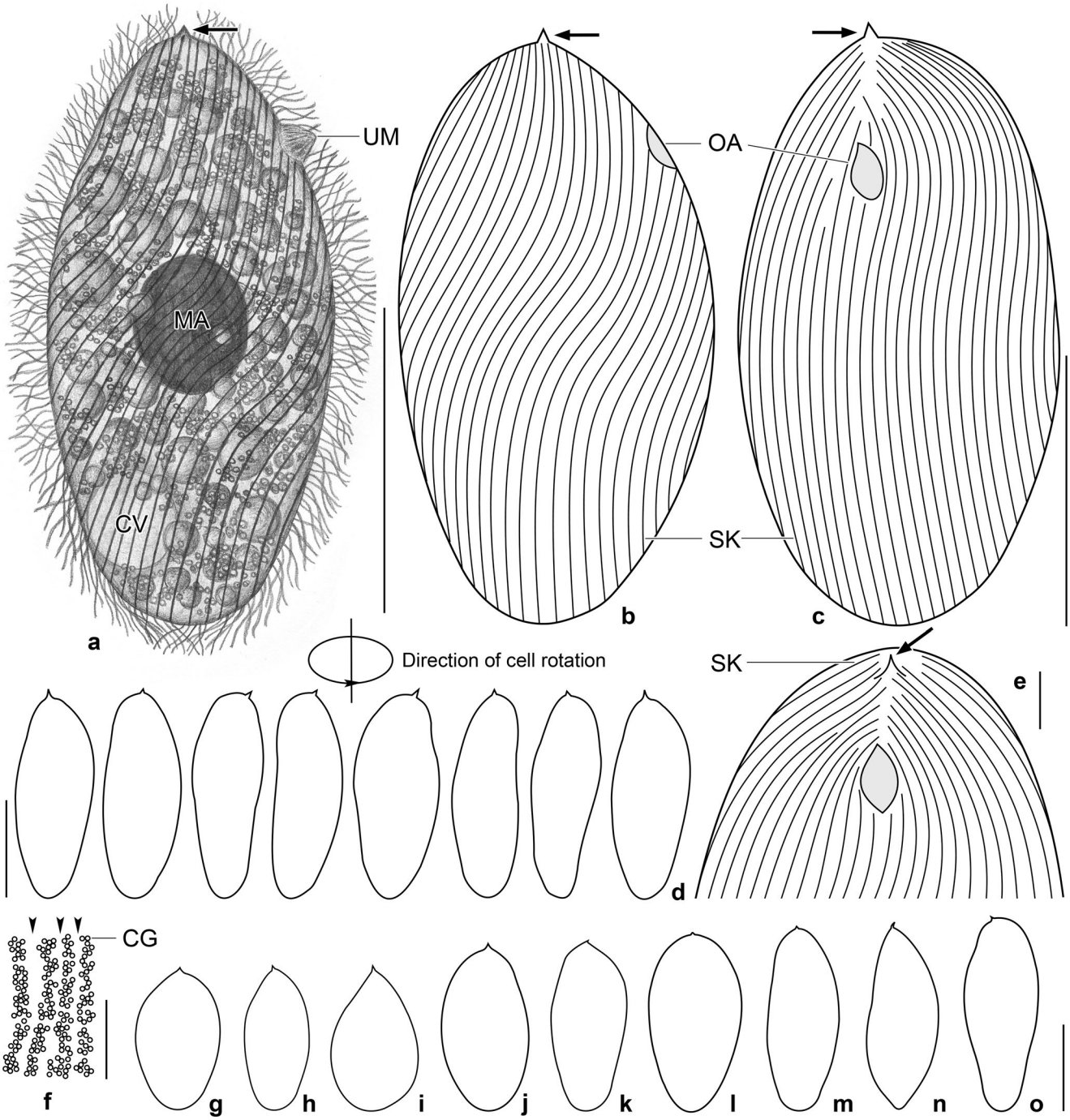

Fig. 1 *Tetrahymena acanthophora* sp. n. from life. **a** Lateral view, showing the ovoid body. The posterior body end is broadly rounded, while the anterior end is notable apiculate (arrow). A single oval macronucleus is located in the central part of the cell. The globular contractile vacuole is subterminal and situated on the dorsal side. The oral apparatus is situated in the anterior body fourth. **b**, **c** Lateral and ventrolateral views, showing the sigmoidal course of somatic kineties. Arrows denote the apiculate anterior cell pole. **d** Schematic sequence of rotating cell during swimming motion. **e** Ventral view of the anterior body third, showing the course of somatic kineties right and left of the oral apparatus. Arrow marks the apiculate anterior body end. **f** Surface view, showing the arrangement of cortical granules between somatic kineties (arrowheads). **g**–**o** Variability of body shape and size of free-swimming specimens. Drawn to scale. *Explanations* = contractile vacuole (*CV*), cortical granules (*CG*), macronucleus (*MA*), oral apparatus (*OA*), somatic kineties (*SK*), undulating membrane (*UM*). *Scale bars* = 5 μm (**f**), 10 μm (**e**), and 50 μm (**a**–**d**, **g**–**o**)

ca. 4 μm long thorn-like structure, whereas the posterior cell pole was narrowly to broadly rounded (Figs. 1a–e, g–o; 2a–f, i, j; and 3a, c). There was a single oval macronucleus situated roughly in the central part of the cell and recognizable only after application of methyl green (Fig. 3a–e). The stained macronucleus measured 11–16 × 9–13 μm and contained a single

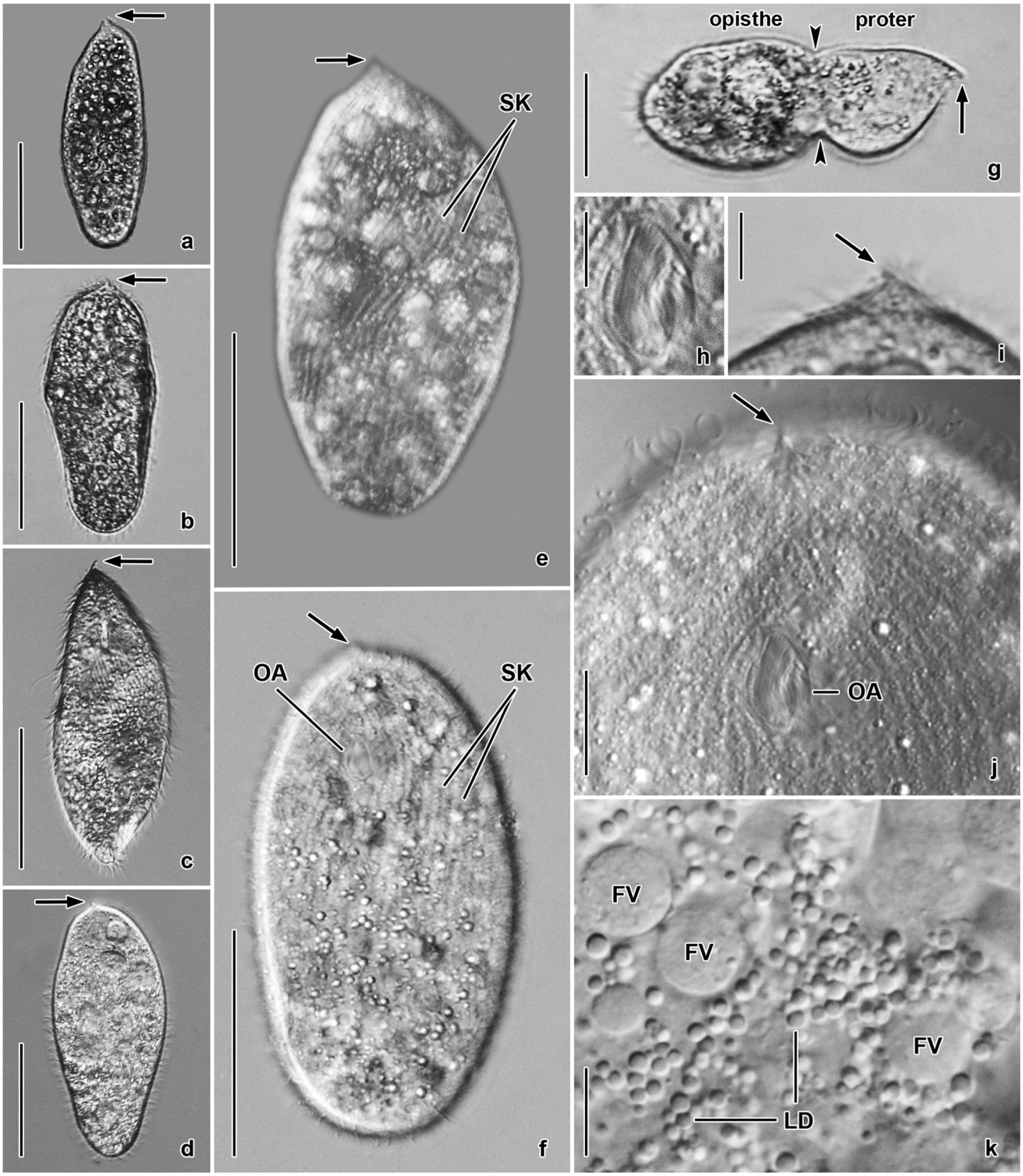

Fig. 2 *Tetrahymena acanthophora* sp. n. from life. **a**–**d** Overviews, showing free-swimming cells. Arrows indicate the apiculate anterior cell pole. **e**, **f** Lateral and ventrolateral views, showing the sigmoidal course of somatic kineties. Arrows point to the apiculate anterior body end. **g** Ventral view of a late divider. Division occurs in freely motile (non-encysted) conditions and binary fission is homothetogenic. Opposed arrowheads mark the division furrow, arrow denotes the apiculate cell pole of the proter. **h** Detail of the oral apparatus whose right side is bordered by an undulating membrane composed of a single row of cilia. **i** Detail of the apiculate anterior body end (arrow). **j** Ventral view of the anterior body third, showing the course of somatic kineties in the area between the apex of the body (arrow) and the oral apparatus. **k** Detail of the cytoplasm, showing several larger food vacuoles and many globular lipid droplets. *Explanations* = food vacuoles (*FV*), lipid droplets (*LD*), oral apparatus (*OA*), somatic kineties (*SK*). *Scale bars* = 5 μm (**h**, **i**), 10 μm (**j**, **k**), and 50 μm (**a**–**g**)

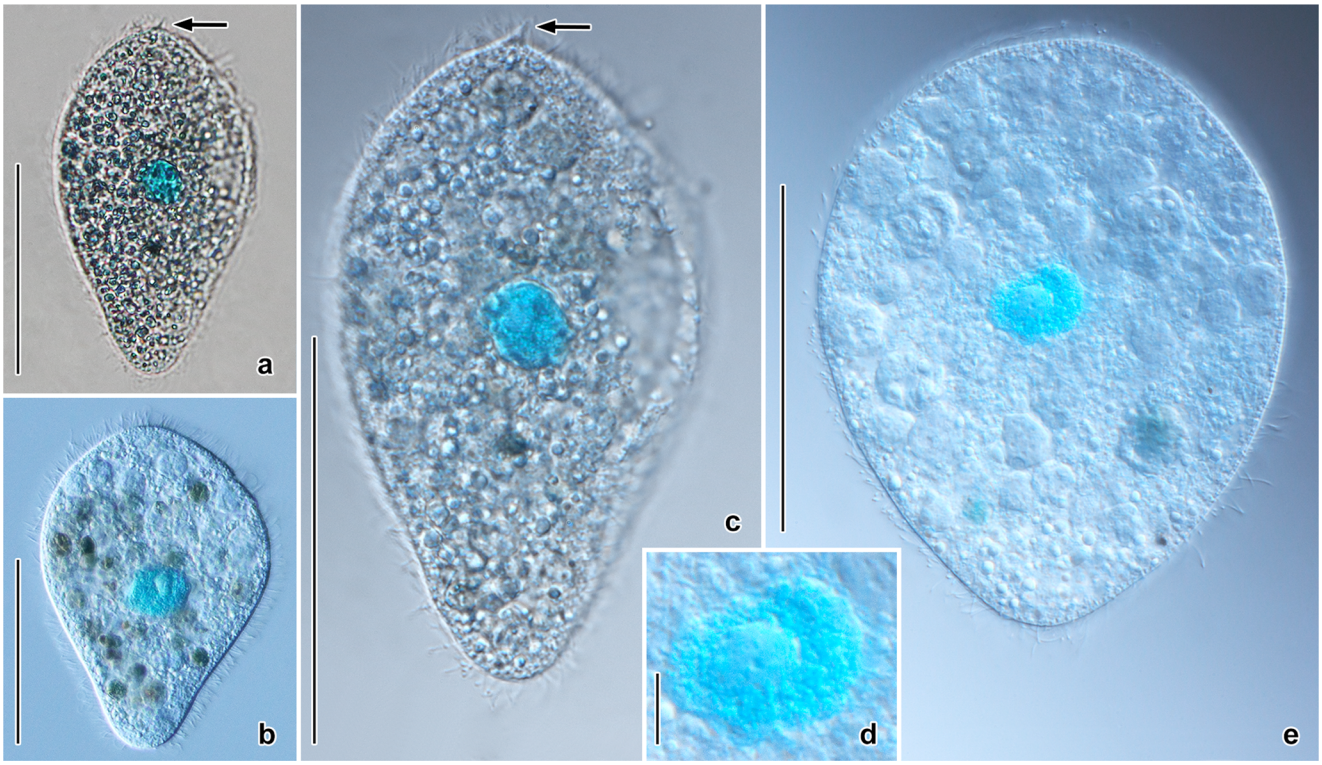

Fig. 3 *Tetrahymena acanthophora* sp. n. after methyl green staining. **a**–**c**, **e** Dorsolateral views, showing the position as well as the shape of the macronucleus. Arrows denote the apiculate anterior cell pole. **d** Detail of the elliptical macronucleus with a single large nucleolus. *Scale bars* = 5 μm (**d**) and 50 μm (**a**–**c**, **e**)

nucleolus being about 6 × 4 μm in size. Micronucleus was not observed either after methyl green or in differential interference contrast optics. One contractile vacuole was located subterminally on the dorsal body side (Fig. 1a). The pulsation cycle of the contractile vacuole took around 18 s. At the beginning of diastole, there were several smaller oval to elliptical vesicles that fused to form a single compact circular vacuole reaching a diameter of about 12 μm at the end of diastole. The cytoplasm was colorless and packed with granules, lipid droplets about 1.3–2.0 μm across, and food vacuoles being up to 7 μm in diameter and containing pieces of host tissues and pigment host cells (Figs. 1a and 2k).

Somatic cilia were about 8.5–10.5 μm long and arranged in 28–30 rows on each side of the cell. Individual rows were approximately 3 μm distant from each other in the mid-body, while only about 1.5 μm at the anterior and posterior cell poles. The course of somatic kineties appeared slightly sigmoidal in lateral view (Figs. 1b, c and 2e). Ventral ciliary rows formed a suture extending from the apical body end to the beginning of the oral apparatus (Figs. 1e and 2j). Between each two somatic kineties, there were cortical granules arranged in two to four staggered and densely spaced rows (Fig. 1f). The movement was elegant by swimming and rotating about the longitudinal body axis.

The oral apparatus was about 20 μm away from the anterior body end. It was tear-shaped and measured only approximately 10 × 6 μm. The right side of the buccal cavity was lined by the paroral membrane whose cilia were ca. 10 μm long and covered the buccal cavity, causing that the adoral organelles could not be recognized in vivo (Figs. 1b–e and 2f–j).

Division occurred in freely motile (non-encysted) conditions and it was homothetogenic (Fig. 2g).

Description of *Tetrahymena nigricans* sp. n.

ZooBank registration number: urn:lsid:zoobank.org:act:B31A3E54-70BF-4A2D-8865-8FDA231DE02B.

Diagnosis: Size about 85 × 65 μm. Body oval with both ends broadly rounded. Contractile vacuole dorsal and in third fourth of body length. Cytoplasm packed with lipid droplets and food vacuoles, causing a dark appearance of cell at low magnifications. About 18 meridional ciliary rows on each body side, no caudal cilia.

Type locality: Veľkobielske jazero lake, recreation area in the village of Veľký Biel, Podunajská rovina plain (48° 12′ 26.4″ N, 17° 21′ 28.3″ E).

Type host: *Girardia tigrina* (Girard, 1850) Ball, 1974.

Type material: A DNA sample of holotype specimen has been deposited in Natural History Museum, Vajanského

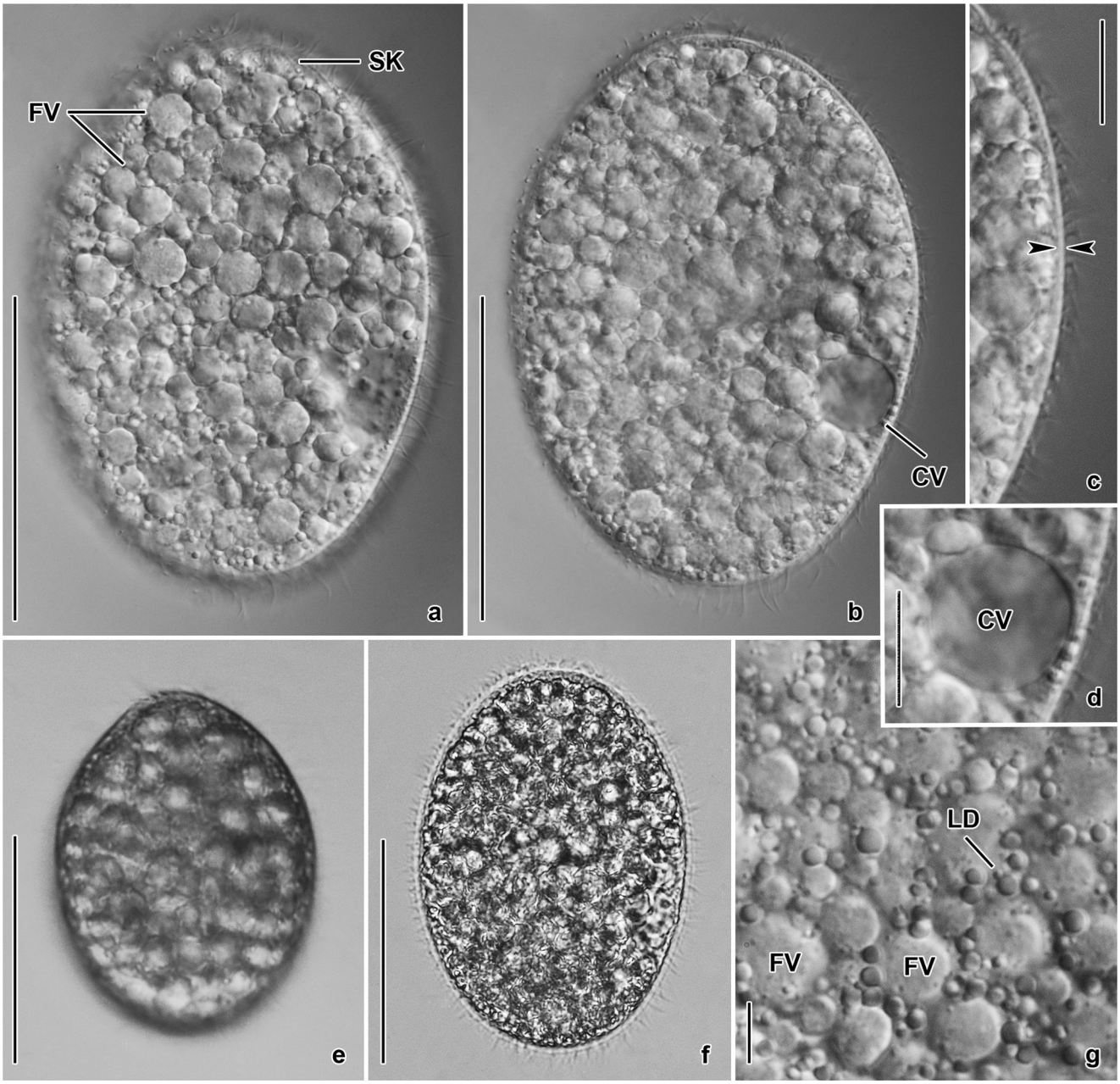

Fig. 4 *Tetrahymena nigricans* sp. n. from life. **a**, **b**, **e**, **f** Lateral overviews, showing the oval body with cytoplasm densely packed with food vacuoles. Note that the contractile vacuole is situated slightly below the mid-body on dorsal body side. **c** Detail of dorsal body margin. Opposed arrows denote the comparatively thick cortex. **d** Detail of globular contractile vacuole during diastole. **g** Detail of cytoplasm, showing larger food vacuoles and smaller lipid droplets. *Explanations* = contractile vacuole (*CV*), food vacuoles (*FV*), lipid droplets (*LD*), somatic kineties (*SK*). *Scale bars* = 5 μm (**g**), 10 μm (**c**, **d**), and 50 μm (**a**, **b**, **e**, **f**)

nábrežie 2, 810 06 Bratislava, Slovakia (ID Collection Code 1427127).

Gene sequences: The nuclear 18S rRNA gene sequence of holotype specimen has been deposited in GenBank (accession no. MN994472). The sequence is 1707 nucleotides long and has a GC content of 43.06%. The mitochondrial 16S rRNA gene sequence of holotype specimen has been deposited in GenBank (accession no. MN994483). The sequence is 991 nucleotides long and has a GC content of 31.08%. The COI gene sequence of holotype specimen has been deposited in GenBank (accession no. MN991323). The sequence is 915 nucleotides long and has a GC content of 25.35%.

Etymology: The specific epithet *nigrican·s*, *–s*, *–s* [m, f, n] (blackish) is a Latin adjective referring to the dark appearance of the species caused by the densely packed cytoplasm with food vacuoles.

Description: Morphological description of this species is considerably limited due to its extremely rare occurrence in planarians. Specifically, only four specimens of *T. nigricans* were detected, two were sampled for molecular analyses and two for in vivo observations. Thus, all measurements were based only on two cells. Unfortunately, the densely packed cytoplasm made observations of most taxonomically important features almost impossible.

The body size was about 75–90 × 55–70 μm in vivo (n = 2). The shape was oval with both poles broadly rounded and did not distinctly change under the coverslip pressure (Fig. 4a–f). The only clearly visible organelle was the contractile vacuole. It was spherical, 12–13 μm in diameter and located dorsally in the third fourth of the body length (Fig. 4b, d). One pulsation cycle from the beginning of systole until the contractile vacuole was fully formed from smaller vesicles took approximately 13 s. The cytoplasm was colorless and packed with a huge amount of food vacuoles being 3.0–7.8 μm in diameter and 1.0–1.7 μm-sized lipid droplets (Fig. 4g). Somatic cilia were about 8.5–9.5 μm long. Based on the spacing of some visible ciliary rows and the width of the anterior body region, it was estimated that there might have been ca. 18 meridional ciliary rows on each side of the cell.

Description of *Tetrahymena dugesiae* sp. n.

2019 *Tetrahymena* sp. – Rataj and Vďačný, Dis Aquat Org 134: 157 (Figs. 3A–H and 4A–K)

ZooBank registration number: urn:lsid:zoobank.org:act:F5F67F43-1FE7-4E98-8BC0-EDD4F1812274.

Fig. 5 Phylogeny based on the concatenated nuclear 18S rRNA gene and mitochondrial COI sequences, showing the systematic position of tetrahymenas isolated from freshwater planarians. Bootstrap values for maximum likelihood (ML) and posterior probabilities for Bayesian inference (BI) were mapped onto the best scoring IQ tree. Dashes indicate mismatch between ML and BI trees. Sequences in bold face were obtained during this study. The strain MP80 was mislabeled as *T. elliotti* by Chantangsi et al. (2007). According to Doerder (2019), *T. elliotti* is related to *T. gruchyi*. For accession numbers, see Supplementary Table S1. The scale bar denotes one substitution per ten nucleotide positions

Diagnosis: Size about 115 × 50 μm. Body narrowly to broadly fusiform with anterior end differentiated into a plate-like rostrum and posterior end broadly rounded. Macronucleus oval. Contractile vacuole dorsal and subterminal. About 10 to 12 meridional ciliary rows on each body side, no caudal cilia. Oral apparatus about 10 μm long.

Type locality: Milošovanský potok stream, inundation area in the vicinity of the village of Milošová, Turzovská vrchovina highlands (49° 28′ 17.1″ N, 18° 45′ 18.4″ E).

Type host: *Dugesia gonocephala* (Dugès, 1830) Girard, 1850.

Type material: A DNA sample of holotype specimen has been deposited in Natural History Museum, Vajanského nábrežie 2, 810 06 Bratislava, Slovakia (ID Collection Code 1425919).

Gene sequences: The nuclear 18S rRNA gene sequence of holotype specimen has been deposited in GenBank (accession no. MK454732). The sequence is 1749 nucleotides long and has a GC content of 43.28%. The mitochondrial 16S rRNA gene sequence of holotype specimen

Table 2 Characterization of new sequences of tetrahymenas isolated from freshwater planarians

Specimen	Site code	Nuclear 18S rRNA gene			Mitochondrial 16S rRNA gene		Cytochrome oxidase subunit I			
		Length (nt)	GC (%)	GenBank entry	Length (nt)	GC (%)	GenBank entry	Length (nt)	GC (%)	GenBank entry
T. acanthophora VB55	13	–	–	–	996	29.92	MN994473	946	25.58	MN991313
T. acanthophora VB56	13	1712	43.11	MN994469	996	29.92	MN994474	946	25.58	MN991314
T. acanthophora JK59	15	1712	43.11	MN994470	996	29.92	MN994475	946	25.58	MN991315
T. acanthophora ZP61	16	1712	43.11	MN994471	996	29.92	MN994476	946	25.58	MN991316
T. acanthophora ZP62	16	–	–	–	996	29.92	MN994477	946	25.58	MN991317
T. dugesiae KD30	1	–	–	–	987	32.21	MN994478	967	24.61	MN991318
T. dugesiae O10	3	–	–	–	987	32.21	MN994479	967	24.61	MN991319
T. dugesiae M17	4	1749	43.28	MK454732[a]	987	32.12	MN994480	967	25.23	MN991320
T. dugesiae PC31	6	–	–	–	987	32.21	MN994481	967	24.61	MN991321
T. dugesiae PC32	6	–	–	–	987	32.21	MN994482	967	24.61	MN991322
T. nigricans VB57	13	1707	43.06	MN994472	991	31.08	MN994483	915	25.35	MN991323
T. scolopax M14	4	–	–	–	1009	30.72	MN994484	967	25.96	MN991324

[a] Sequence obtained in our previous study (Rataj and Vďačný 2019)

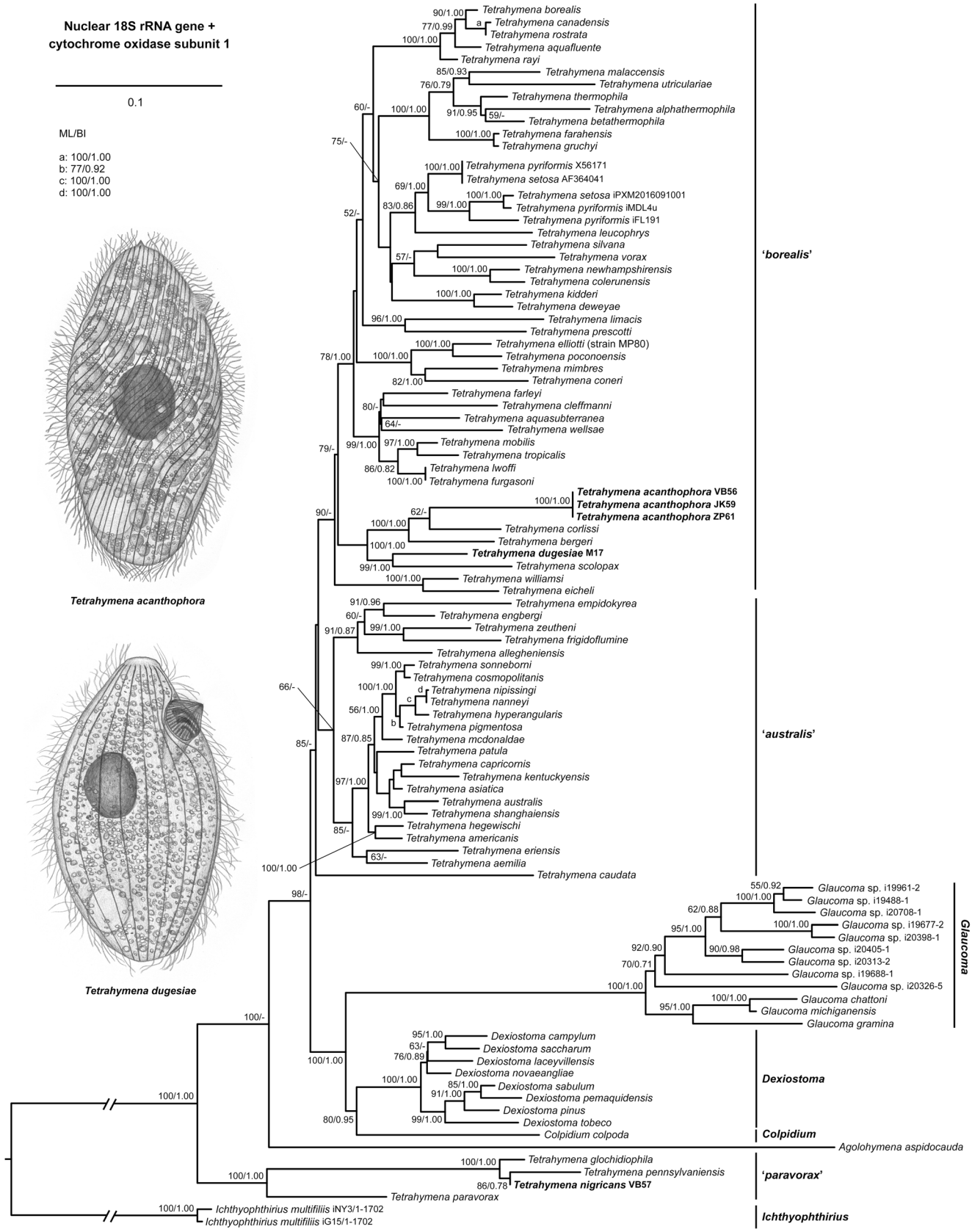
Nuclear 18S rRNA gene + cytochrome oxidase subunit 1
0.1
ML/BI
a: 100/1.00
b: 77/0.92
c: 100/1.00
d: 100/1.00
Tetrahymena acanthophora
Tetrahymena dugesiae
Tetrahymena borealis
Tetrahymena canadensis
Tetrahymena rostrata
Tetrahymena aquafluente
Tetrahymena rayi
Tetrahymena malaccensis
Tetrahymena utriculariae
Tetrahymena thermophila
Tetrahymena alphathermophila
Tetrahymena betathermophila
Tetrahymena farahensis
Tetrahymena gruchyi
Tetrahymena pyriformis X56171
Tetrahymena setosa AF364041
Tetrahymena setosa iPXM2016091001
Tetrahymena pyriformis iMDL4u
Tetrahymena pyriformis iFL191
Tetrahymena leucophrys
Tetrahymena silvana
Tetrahymena vorax
Tetrahymena newhampshirensis
Tetrahymena colerunensis
Tetrahymena kidderi
Tetrahymena deweyae
Tetrahymena limacis
Tetrahymena prescotti
Tetrahymena elliotti (strain MP80)
Tetrahymena poconoensis
Tetrahymena mimbres
Tetrahymena coneri
Tetrahymena farleyi
Tetrahymena cleffmanni
Tetrahymena aquasubterranea
Tetrahymena wellsae
Tetrahymena mobilis
Tetrahymena tropicalis
Tetrahymena lwoffi
Tetrahymena furgasoni
Tetrahymena acanthophora VB56
Tetrahymena acanthophora JK59
Tetrahymena acanthophora ZP61
Tetrahymena corlissi
Tetrahymena bergeri
Tetrahymena dugesiae M17
Tetrahymena scolopax
Tetrahymena williamsi
Tetrahymena eicheli
'borealis'
Tetrahymena empidokyrea
Tetrahymena engbergi
Tetrahymena zeutheni
Tetrahymena frigidoflumine
Tetrahymena allegheniensis
Tetrahymena sonneborni
Tetrahymena cosmopolitanis
Tetrahymena nipissingi
Tetrahymena nanneyi
Tetrahymena hyperangularis
Tetrahymena pigmentosa
Tetrahymena mcdonaldae
Tetrahymena patula
Tetrahymena capricornis
Tetrahymena kentuckyensis
Tetrahymena asiatica
Tetrahymena australis
Tetrahymena shanghaiensis
Tetrahymena hegewischi
Tetrahymena americanis
Tetrahymena eriensis
Tetrahymena aemilia
Tetrahymena caudata
'australis'
Glaucoma sp. i19961-2
Glaucoma sp. i19488-1
Glaucoma sp. i20708-1
Glaucoma sp. i19677-2
Glaucoma sp. i20398-1
Glaucoma sp. i20405-1
Glaucoma sp. i20313-2
Glaucoma sp. i19688-1
Glaucoma sp. i20326-5
Glaucoma chattoni
Glaucoma michiganensis
Glaucoma gramina
Glaucoma
Dexiostoma campylum
Dexiostoma saccharum
Dexiostoma laceyvillensis
Dexiostoma novaeangliae
Dexiostoma sabulum
Dexiostoma pemaquidensis
Dexiostoma pinus
Dexiostoma tobeco
Dexiostoma
Colpidium colpoda
Colpidium
Agolohymena aspidocauda
Tetrahymena glochidiophila
Tetrahymena pennsylvaniensis
Tetrahymena nigricans VB57
Tetrahymena paravorax
'paravorax'
Ichthyophthirius multifiliis iNY3/1-1702
Ichthyophthirius multifiliis iG15/1-1702
Ichthyophthirius

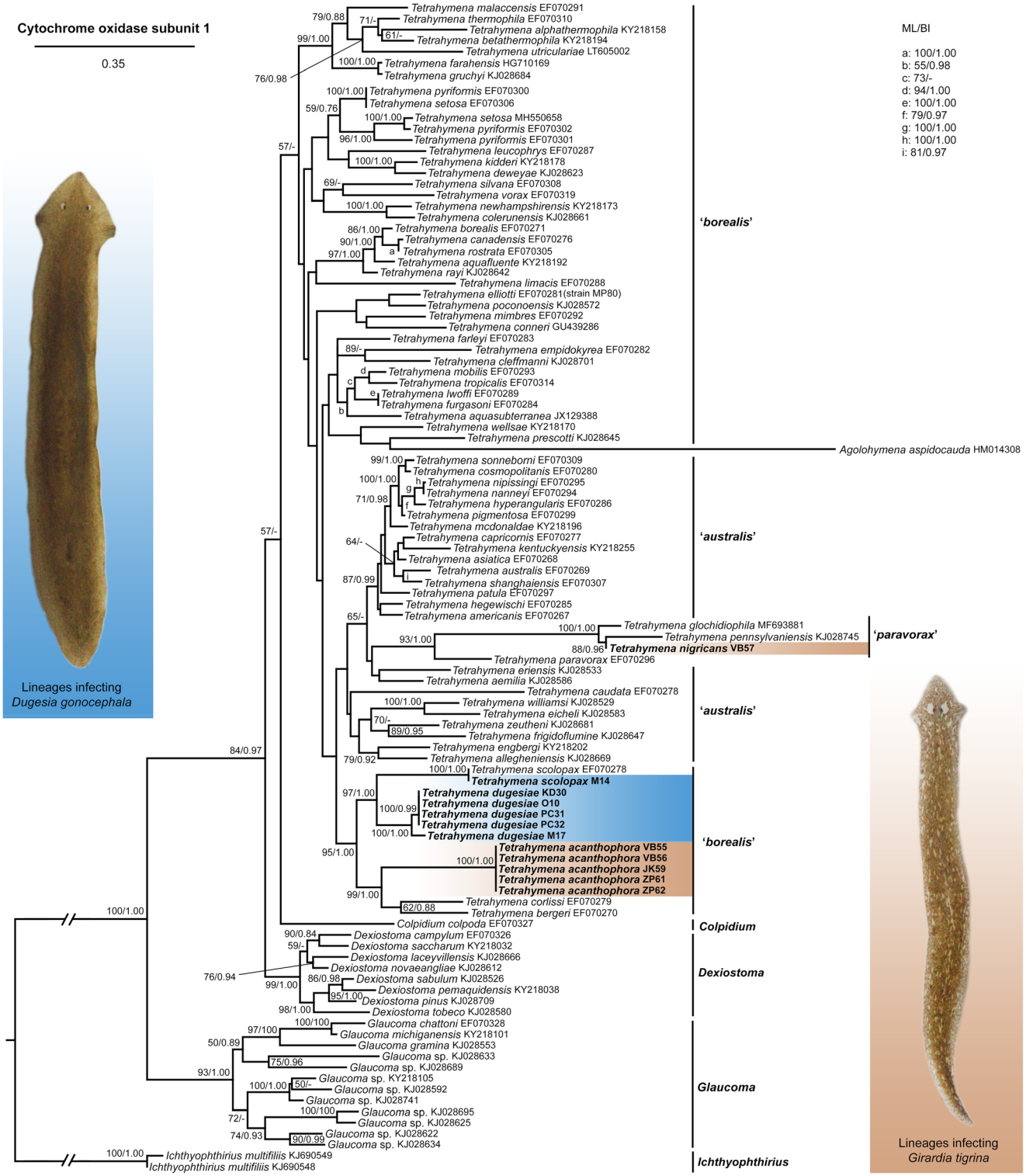

Fig. 6 Phylogeny based on the mitochondrial COI sequences, showing the systematic position of tetrahymenas isolated from freshwater planarians. Bootstrap values for maximum likelihood (ML) and posterior probabilities for Bayesian inference (BI) were mapped onto the best scoring IQ tree. Dashes indicate mismatch between ML and BI trees. Sequences in bold face were obtained during this study. The strain MP80 was mislabeled as *T. elliotti* by Chantangsi et al. (2007). The scale bar denotes 35 substitutions per hundred nucleotide positions

has been deposited in GenBank (accession no. MN994480). The sequence is 987 nucleotides long and has a GC content of 31.12%. The COI gene sequence of holotype specimen has been deposited in GenBank (accession no. MN991320). The sequence is 967 nucleotides long and has a GC content of 25.23%.

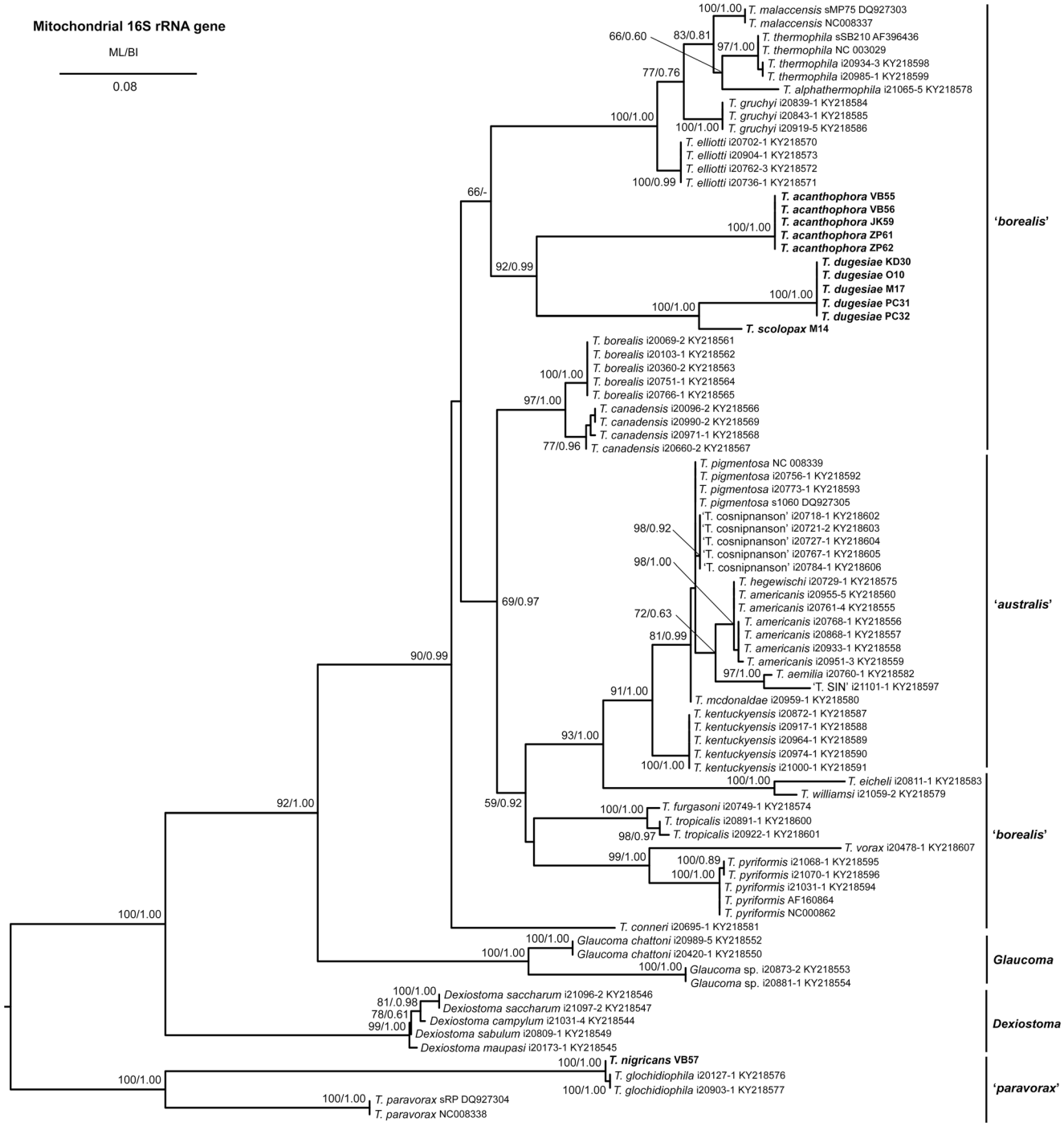

Fig. 7 Phylogeny based on the mitochondrial 16S rRNA gene sequences, showing the systematic position of tetrahymenas isolated from freshwater planarians. Bootstrap values for maximum likelihood (ML) and posterior probabilities for Bayesian inference (BI) were mapped onto the best scoring IQ tree. Dashes indicate mismatch between ML and BI trees. Sequences in bold face were obtained during this study. The scale bar denotes eight substitutions per hundred nucleotide positions

Etymology: The specific epithet *dugesiae* (from *Dugesia*) is a singular genitive case of the Latin noun *Dugesi·a*, *–ae* [f]. It refers to the presence of this ciliate exclusively in *Dugesia* specimens. According to Article 11.9.1.4. of the International Commission on Zoological Nomenclature (1999), the species-group name is to be treated as an adjective used as a substantive in the genitive case, because of its derivation from the host's generic name.

Description: Morphological description is provided in Rataj and Vďačný (2019).

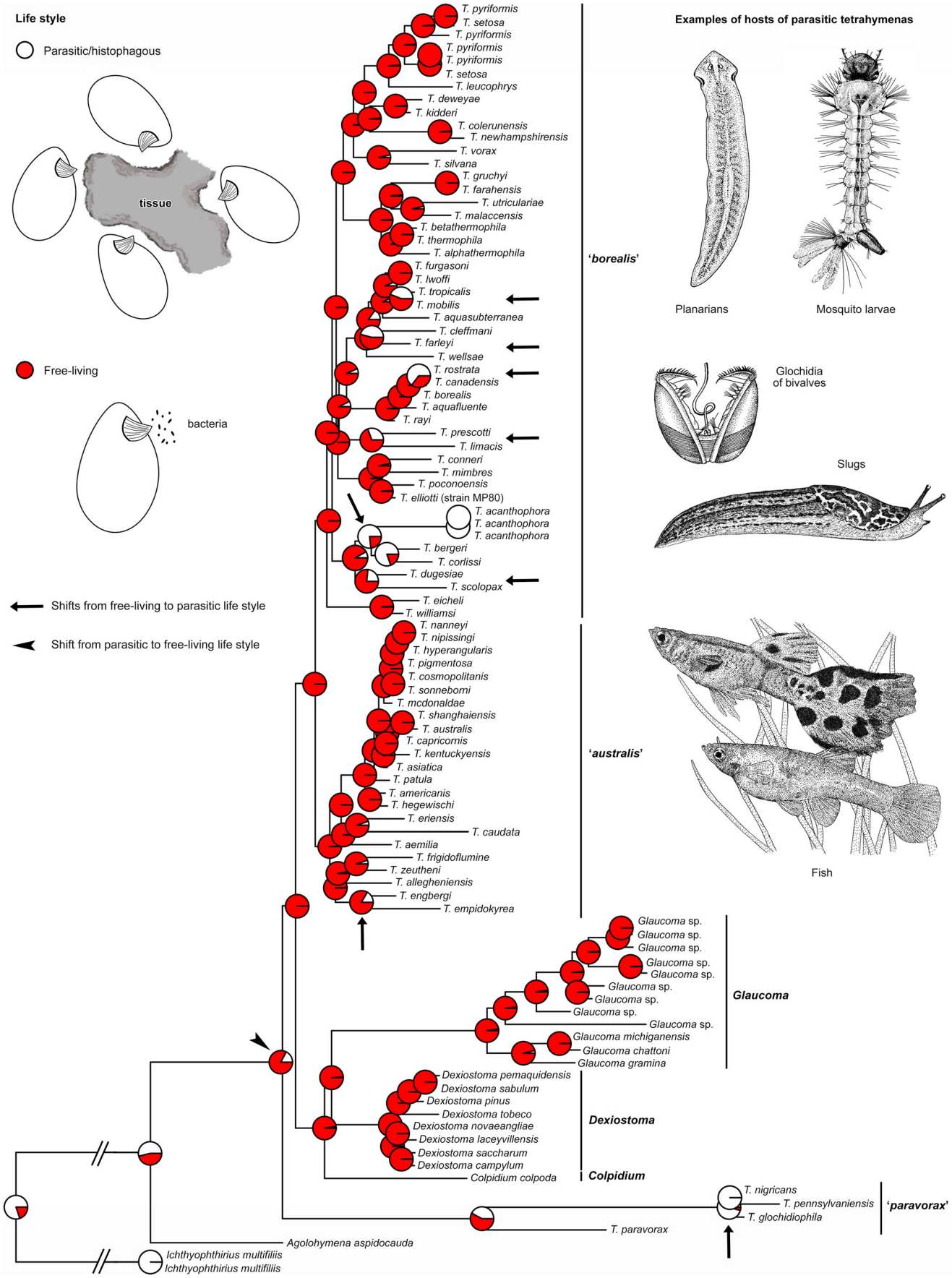
Life style
Parasitic/histophagous
tissue
Free-living
bacteria
Shifts from free-living to parasitic life style
Shift from parasitic to free-living life style
T. pyriformis
T. setosa
T. pyriformis
T. pyriformis
T. pyriformis
T. setosa
T. leucophrys
T. deweyae
T. kidderi
T. colerunensis
T. newhampshirensis
T. vorax
T. silvana
T. gruchyi
T. farahensis
T. utricullariae
T. malaccensis
T. betathermophila
T. thermophila
T. alphathermophila
T. furgasoni
T. lwoffi
T. tropicalis
T. mobilis
T. aquasubterranea
T. cleffmani
T. farleyi
T. wellsae
T. rostrata
T. canadensis
T. borealis
T. aquafluente
T. rayi
T. prescotti
T. limacis
T. conneri
T. mimbres
T. poconoensis
T. elliotti (strain MP80)
T. acanthophora
T. acanthophora
T. acanthophora
T. bergeri
T. corlissi
T. dugesiae
T. scolopax
T. eicheli
T. williamsi
'borealis'
T. nanneyi
T. nipissingi
T. hyperangularis
T. pigmentosa
T. cosmopolitanis
T. sonneborni
T. mcdonaldae
T. shanghaiensis
T. australis
T. capricornis
T. kentuckyensis
T. asiatica
T. patula
T. americanis
T. hegewischi
T. eriensis
T. caudata
T. aemilia
T. frigidoflumine
T. zeutheni
T. allegheniensis
T. engbergi
T. empidokyrea
'australis'
Glaucoma sp.
Glaucoma sp.
Glaucoma sp.
Glaucoma sp.
Glaucoma sp.
Glaucoma sp.
Glaucoma sp.
Glaucoma sp.
Glaucoma michiganensis
Glaucoma chattoni
Glaucoma gramina
Glaucoma
Dexiostoma pemaquidensis
Dexiostoma sabulum
Dexiostoma pinus
Dexiostoma tobeco
Dexiostoma novaeangliae
Dexiostoma laceyvillensis
Dexiostoma saccharum
Dexiostoma campylum
Dexiostoma
Colpidium colpoda
Colpidium
T. nigricans
T. pennsylvaniensis
T. glochidiophila
'paravorax'
T. paravorax
Agolohymena aspidocauda
Ichthyophthirius multifiliis
Ichthyophthirius multifiliis
Examples of hosts of parasitic tetrahymenas
Planarians
Mosquito larvae
Glochidia of bivalves
Slugs
Fish

◀ **Fig. 8** SIMMAP reconstruction of ancestral life strategies based on a set of 1000 randomly selected trees from the posterior distribution of the Bayesian analysis of the concatenated nuclear 18S rRNA gene and mitochondrial COI dataset. Relative proportions of character states were mapped onto the Bayesian 50% majority-rule consensus tree

Phylogenetic analyses

In the present study, we obtained altogether 28 new sequences of three molecular markers belonging to the three new *Tetrahymena* species and *T. scolopax*. Their length, guanine–cytosine content, and GenBank accession numbers are summarized in Table 2. Intraspecies sequence similarities in the 16S and 18S rRNA genes as well as in the COI gene are 100%, except for the single *T. dugesiae* M17 isolate which differs by 0.2% in the 16S rRNA gene and by 2.3% in the COI sequences from the four other conspecific isolates. The COI sequences of Slovak and American isolates of *T. scolopax* are 100% identical.

To assess the phylogenetic position of the newly described tetrahymenas, Bayesian and ML analyses were conducted (Figs. 5, 6, and 7 and Supplementary Fig. S1). Tetrahymenas isolated from planarians were consistently classified within the same clusters across all phylogenetic analyses, even when the overall tree topologies slightly differed depending on the molecular marker(s) and the dataset analyzed. Specifically, *T. acanthophora*, *T. dugesiae*, and *T. scolopax* always formed a group together with *T. bergeri* and *T. corlissi* within the variably supported "*borealis*" clade. *Tetrahymena dugesiae* was consistently depicted as sister to *T. scolopax* with usually full statistical support across all analyses. These two species were shown in a sister relationship with *T. acanthophora* when *T. bergeri* and *T. corlissi* were not included into the analyses (Fig. 7). In datasets, where all three latter species were present, *T. dugesiae* and *T. scolopax* formed their sister clade (Figs. 5 and 6). Relationships among *T. acanthophora*, *T. bergeri*, and *T. corlissi* could not be, however, reliably resolved. On the other hand, *T. nigricans* was in every scenario a part of the "*paravorax*" clade. This cluster was nested within the "*australis*" clade although without any statistical support in COI trees (Fig. 6), while it was placed outside the "core" of the genus *Tetrahymena* in analyses of the concatenated 18S rRNA gene + COI dataset (Fig. 5) and the mitochondrial 16S rRNA gene (Fig. 7). Nevertheless, the internal structure of the *paravorax* clade was consistent across all analyses. *Tetrahymena paravorax* Corliss, 1957 was sister to the branch leading to *T. glochidiophila*, *T. nigricans*, and *T. pennsylvaniensis* Doerder, 2019 (Figs. 5, 6, and 7). Moreover, phylogenetic analyses suggested a closer relationship of *T. nigricans* to *T. pennsylvaniensis* than to *T. glochidiophila* but only with poor statistical support (Figs. 5 and 6).

Reconstructions of ancestral life strategies indicated that the last common progenitor of hymenostomes led a parasitic way of life (Fig. 8). Very likely there were two independent shifts to a free-living strategy, i.e., at the base of the "*paravorax*" clade and in the last common ancestor of *Colpidium* Stein, 1860, *Dexiostoma* Jankowski, 1968, *Glaucoma* Ehrenberg, 1830, and the "core" tetrahymenas ("*australis*" + "*borealis*" clade). Or this transfer might have happened only once at the base of these two clades (Fig. 8, arrowhead), depending on the tree topology, especially, on the phylogenetic position of the histophagous *Agolohymena aspidocauda* Bourland and Strüder-Kypke, 2010. The SIMMAP analyses suggested at least seven independent shifts back to parasitism: (i) in *T. glochidiophila* and *T. nigricans* within the "*paravorax*" clade; (ii) in *T. empidokyrea* within the

Table 3 Fitting of five BiSSE models for parasitic/histophagous (subscript 0) and free-living (subscript 1) hymenostomes, using the program BayesRate

Speciation rate	Extinction rate	Transition rate	log L_M	BF	λ_0	λ_1	μ_0	μ_1	q_{01}	q_{10}
Free	*Free*	*Free*	*− 153.27*	*0.00*	*1.43 ± 5.88*	*0.96 ± 1.03*	*0.46 ± 4.04*	*0.15 ± 0.52*	*0.34 ± 0.28*	*0.26 ± 0.25*
Free	Free	Constrained	− 156.26	5.98	1.33 ± 5.20	0.97 ± 0.99	0.44 ± 3.35	0.16 ± 0.54	0.29 ± 0.29	0.29 ± 0.29
Free	Constrained	Free	− 167.08	27.62	0.74 ± 1.68	1.07 ± 1.09	0.13 ± 0.53	0.13 ± 0.53	0.32 ± 0.27	0.25 ± 0.24
Constrained	Free	Free	− 1.30e13	2.59e13	0.98 ± 0.89	0.98 ± 0.89	0.38 ± 0.52	0.20 ± 0.65	0.32 ± 0.25	0.24 ± 0.25
Constrained	Constrained	Constrained	− 170.16	33.78	0.96 ± 0.90	0.96 ± 0.90	0.20 ± 0.55	0.20 ± 0.55	0.25 ± 0.26	0.25 ± 0.26

The BiSSE models involve six parameters: two speciation rates λ_0 and λ_1 (rate when the lineage is in state 0, i.e., it is parasitic/histophagous, and rate when in state 1, i.e., free-living), two extinction rates μ_0 and μ_1 (when in state 0, and in state 1), and two rates of character state change q_{01} and q_{10} (from 0 to 1, and from 1 to 0). The program BayesRate estimates the six model's parameters and the probabilities that a lineage beginning with state 0 or 1 would evolve into a clade like that observed to have descended from node *N*. These probabilities are tracked back toward the root, accounting for all possible events that could have happened along the way. BayesRate also allows to perform hypothesis tests by variously constraining the six parameters, e.g., is the rate of speciation elevated for one character state over the other (speciation rate free, $\lambda_0 \neq \lambda_1$) or is the speciation rate equal for both character states (speciation rate constrained, $\lambda_0 = \lambda_1$)?

Tabulated are medians of speciation (λ), extinction (μ), and transition (q) rates ± interquartile range estimated over 1000 trees from the posterior distribution of the Bayesian analysis of the first concatenated dataset

BayesFactors (BF) are expressed relative to the model of highest marginal log likelihood (log L_M). Best fitting model is in italic face

"*australis*" clade; and (iii–vii) in *T. mobilis* (Kahl, 1926) Lynn and Doerder, 2012, *T. farleyi* Lynn et al., 2000, *T. limacis*, *T. rostrata* as well as in the *T. acanthophora* + *T. bergeri* + *T. corlissi* + *T. dugesiae* + *T. scolopax* cluster within the "*borealis*" clade (Fig. 8, arrows).

The comparison of log marginal likelihoods of various binary-state speciation and extinction (BiSSE) models for diversification of parasitic and free-living hymenostomes indicated that the model with all parameters free is to be preferred over models where speciation, extinction, and transition rates were constrained (Table 3). The subsequent MCMC simulations suggested that the free-living hymenostome lineages have a distinctly higher speciation rate than the parasitic lineages (Fig. 9, left upper panel). Although the extinction rate between the two types of lineages overlapped significantly, the parasitic branches appear to be subjected to even a much higher risk of becoming extinct (Fig. 9, right upper panel). Consequently, the net diversification rate of the free-living lineages was revealed to be distinctly higher than in the parasitic ones (Fig. 9, left lower panel). As concerns the transition rates, the estimated values distinctly overlapped, although the q_{01} rate seemed to be higher (Fig. 9, right lower panel). This conspicuous overlap was very likely the reason why the best fitting model did not receive strong evidence (BF < 6.0) against the model with q_{01} and q_{10} constrained to be equal (Table 3). In turn, this indicates that both transition rates might have not been different and hence transfers from the free-living to the parasitic strategy and vice versa are equally probable in hymenostome ciliates.

Discussion

The three new *Tetrahymena* species

In the present study, we have introduced three species of *Tetrahymena* which undoubtedly represent new taxa also with respect to the ciliate-description recommendations proposed by Warren et al. (2017). However, because most species in this genus lack morphologically unique features, erection of new forms based solely on morphological characteristics is impossible (Lynn et al. 2018). Therefore, the distinctness of Slovak isolates was grounded, especially, on three molecular markers including the 16S and 18S rRNA genes as well as the barcoding COI gene, following Doerder (2019). In their detailed tribute to ciliate taxonomy, Warren et al. (2017) also stated that the genetic divergence cannot serve as an indisputable tool for species identification only by itself due to the absence of one generally accepted threshold value for every molecular marker utilized. Nevertheless, it was already shown that tetrahymenas exhibit an average of about 10.5% interspecific genetic divergence in the barcoding region of their COI sequences, while less than 1% intraspecific variability in this region (Chantangsi et al. 2007). Nevertheless, Doerder (2014, 2019) used a 4% interspecific divergence threshold and mentioned exceptions to the 1% intraspecific variability rule. The threshold proposed by Chantangsi et al. (2007) holds for tetrahymenas infecting planarians and belonging to the "*borealis*" clade. Specifically, the COI pairwise differences between *T. acanthophora*, *T. dugesiae*, and their closest relatives, *T. corlissi*, *T. bergeri*, and *T. scolopax*, were consistently ~ 11%. *Tetrahymena acanthophora* and *T. dugesiae* were also depicted as very distinct branches in all phylogenetic trees (Figs. 5, 6, and 7 and Supplementary Fig. S2). Moreover, the conspicuous thorn situated at the anterior body pole together with the uniquely sigmoidally arranged somatic kineties make *T. acanthophora* to be comparatively easily morphologically distinguishable already by detailed in vivo examination. The only other *Tetrahymena* species with a distinctly apiculate anterior end is the parasitic stage of *T. limacis* (Brooks 1968; Kozloff 1946). However, its ciliary rows are arranged meridionally, as usual in the genus *Tetrahymena*. In addition, our phylogenetic analyses also document that *T. acanthophora* and *T. limacis* are phylogenetically distant (Figs. 5 and 6), whereby their COI sequences share only 85% identity. The detailed morphological comparison of *T. dugesiae* with its closest relatives is provided in Rataj and Vďačný (2019).

As concerns the third new species proposed here, *T. nigricans* undoubtedly belongs to the "*paravorax*" clade. Interestingly, the degree of 18S rRNA and COI sequence identities differs considerably among the members of this group. Unlike the cluster containing *T. acanthophora* and *T. dugesiae* whose 18S rRNA gene sequences differ by 0.3–1.2%, *T. glochidiophila*, *T. pennsylvaniensis*, and *T. nigricans*, all belonging to the "*paravorax*" clade, share completely identical 18S rRNA gene sequences. Even though *T. nigricans* appears in a closer relationship with the free-living *T. pennsylvaniensis* than with the parasitic *T. glochidiophila* (Figs. 5 and 6), the COI sequence of *T. nigricans* is more similar to that of *T. glochidiophila* (5.4% divergence) than to that of *T. pennsylvaniensis* (7.2% divergence). This along with the identical 18S rRNA gene sequences indicates a rather recent origin and rapid radiation of *T. glochidiophila*, *T. pennsylvaniensis*, and *T. nigricans* driven by adaptive changes in new ecological situations. The former two species have been so far reported only from North America, *T. glochidiophila* is a parasite of glochidia and *T. pennsylvaniensis* is free-living (Doerder 2019; Lynn et al. 2018). We have detected *T. nigricans* in the planarian *G. tigrina* which is native to North America (Ball 1974) and was introduced into many European countries and Japan with aquatic plants (Dahm 1958; Kawakatsu et al. 1985), possibly also with its ciliate parasite. Although detailed morphological data are available only for *T. glochidiophila* (Lynn et al. 2018)

and the morphological description of *T. nigricans* is considerably limited, both species are very dissimilar already at first glance. *Tetrahymena nigricans* is much bigger and has an oval body with both poles broadly rounded, while *T. glochidiophila* is only about half of its size and has an ovoid body with anterior pole notably tapered. Moreover, *T. glochidiophila* possesses a prominent oral apparatus and its bacterivorous form bears a single caudal cilium. None of these features were recognized in our isolate. Both species differ also by the location of the contractile vacuole which is situated subterminally in *T. glochidiophila*, while slightly below the mid-body in *T. nigricans*. Moreover, *T. nigricans* is a parasite of planarians, while *T. glochidiophila* attacks glochidia of bivalves. Even though the COI divergence is below the 10% threshold, *T. glochidiophila* and *T. nigricans* are highly morphologically and ecologically dissimilar, which justifies their species status.

As mentioned above, the three new species can be differentiated from their nearest relatives also by detailed in vivo observations. Nevertheless, it is important to mention some problems that might arise during the morphological identification. First, the morphological properties of cultured cells might differ from those freshly isolated from the host, as it has been documented for the parasitic *T. limacis* (for a review, see Corliss 1973). Second, it cannot be excluded that the three new species might have also free-living forms, as indicated by the detection of *T. scolopax* both in *D. gonocephala* (present study) and in freshwater (Doerder 2019). Because there is no guarantee that morphologies of parasitic and free-living forms are similar, the identification needs to be proven also by molecular data. Finally, since our morphological data are based only on freshly isolated living cells, we had difficulties to recognize the micronucleus, which represents an important taxonomic character (Doerder 2014). Whether the tree new species are amicronucleates needs to be therefore confirmed by protargol impregnation, DAPI staining, and/or detailed observations of mid-dividers in which the division spindle of the micronucleus is well recognizable.

Diversity of tetrahymenas infecting planarians

Despite our extensive sampling effort, we isolated altogether only four *Tetrahymena* species and they were found only in two out of the eight freshwater planarian species studied, namely, in *Dugesia gonocephala* and *Girardia tigrina*. On the other hand, Wright (1981) recorded *Tetrahymena* infections in populations of *Crenobia alpina*, *Polycelis felina*, and *Phagocata vitta* (Dugès, 1830) Leidy, 1847 in North Wales. The two former planarian species were *Tetrahymena*-free in our samples and the latter species was not found during material collection in Slovakia. Wright (1981) mentioned that ciliates from *C. alpina* were identified as *T. pyriformis* based on silver preparations. He further stated that *T. corlissi* was also detected in some *C. alpina* individuals from East Anglia. Unfortunately, no DNA of these tetrahymenas was isolated and, therefore, their specificity cannot be tested with modern molecular phylogenetic methods. Apart from Wright's (1981) reports, it seems that *T. pyriformis* was also responsible for some infections of *Dendrocoelum lacteum* (Wright 1969). Considering that this *Tetrahymena* species was present not only in freshwater planarians (e.g., Antipa and Small 1971; Nekuie Fard et al. 2011), we assume that it does not prefer one specific type of triclads but a rather wide spectrum of accessible hosts. Indeed, tetrahymenas very likely show a weak structural/phylogenetic host specificity (Rataj and Vďačný 2019; Strüder-Kypke et al. 2001). However, this needs to be also confirmed by much more extensive molecular data, because all new tetrahymenas described in this study turned out to be confined to a certain planarian species. Even though the prevalence of tetrahymenas in *D. gonocephala* and *G. tigrina* was very low (ranging from ~ 1 to 10.3%), the infections were never coincidental. Specifically, all three new tetrahymenas were recorded at multiple collection sites and tetrahymenas isolated from *G. tigrina* were never found to feed on *D. gonocephala* and vice versa. Both planarians are also ecologically different and very likely do not meet in nature. The former species lives in stagnant water bodies, while the latter is restricted to running waters.

Whether the presence of *T. scolopax* in a single planarian sample was accidental, remains to be further studied as we have detected it only once. The type locality of *T. scolopax* is the Woodcock Creek in Pennsylvania, USA (Doerder 2019). Unfortunately, we have not examined water samples from the site where infected planarians were detected. Since Doerder (2019) found free-living forms of species also reported as parasites, further investigations are needed to corroborate whether *T. scolopax* is an obligate or a facultative parasite of aquatic animals, having both free-living and parasitic stages. In the present study, *T. scolopax* co-occurred with *T. dugesiae* in *D. gonocephala*. This is not very surprising, since mixed *Tetrahymena* infections were already observed in gray garden slug (Brooks 1968).

To summarize, the present study and literature data (Reynoldson and Bellamy 1973; Wright 1981) indicate that 25% of planarian species are positive for *Tetrahymena*. The prevalence of *Tetrahymena* infections ranges from about 1 to ~ 10%. Out of the four *Tetrahymena* species found during the present study, three were recognized to be new taxa. This indicates a large undescribed ciliate diversitylinking histone acetylation to gene activation in freshwater planarians. Nevertheless, six species have been so far reported to infect planarians: *T. acanthophora*, *T. corlissi*, *T. dugesiae*, *T. nigricans*, *T. pyriformis*, and *T. scolopax*. The identity of *T. corlissi* and *T. pyriformis* needs to be supported by

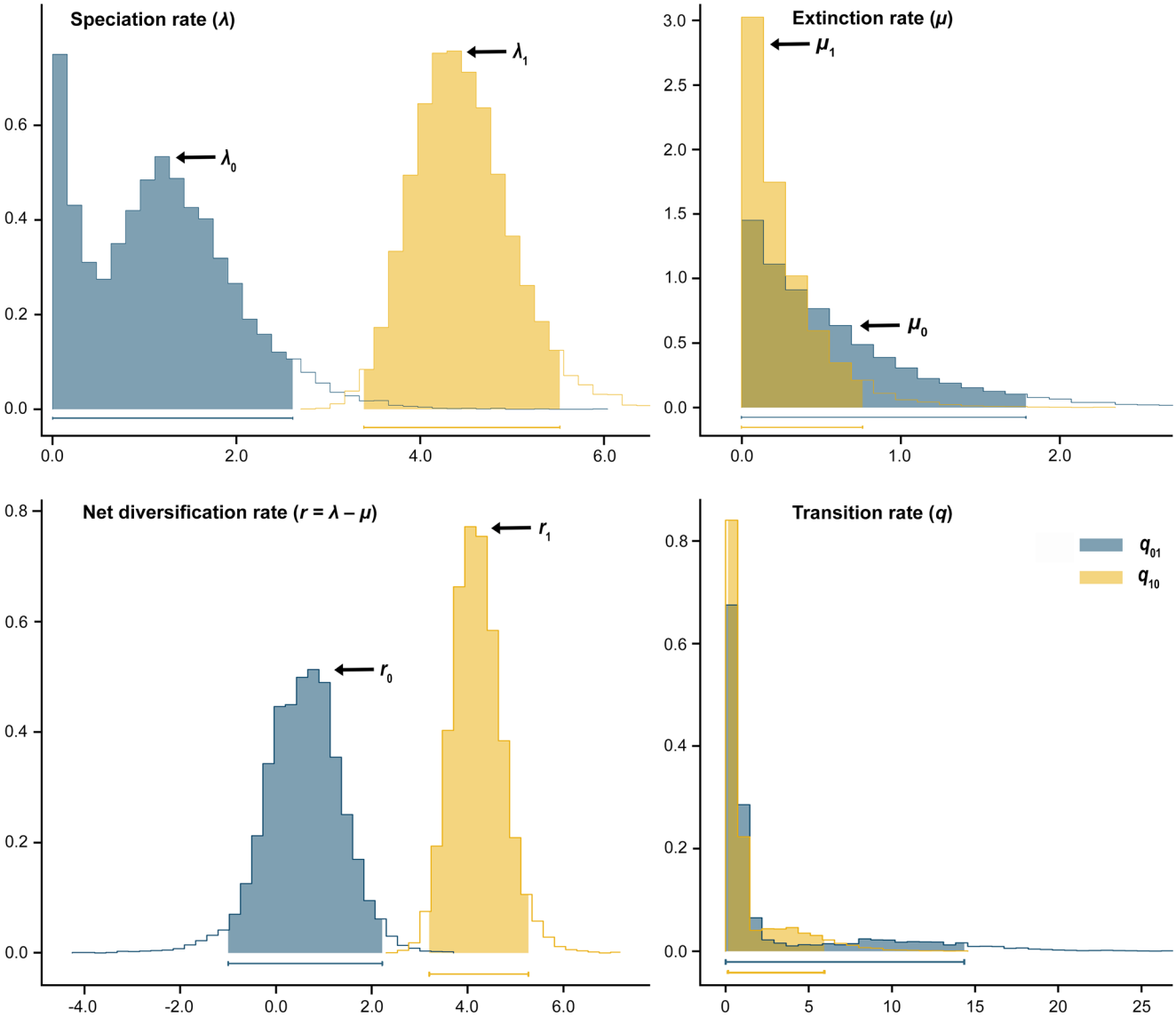

Fig. 9 Posterior densities of speciation rate λ, extinction rate μ, net diversification rate r as well as of transition rate q of parasitic (subscript 0, blue color) and free-living (subscript 1, yellow color) hymenostome lineages. Ninety-five percent intervals are indicated below posterior densities

molecular data. We believe that intensive research on insufficiently explored or completely neglected planarians might still reveal new *Tetrahymena* species.

Evolution of life strategies in *Tetrahymena*

The ancestral way of life in hymenostome ciliates has been analyzed in two previous studies, using the parsimony framework (Rataj and Vďačný 2019; Strüder-Kypke et al. 2001). However, both reconstructions were not unequivocal for the node of the "core" Tetrahymenidae Corliss, 1952 and, therefore, it was not possible to state whether the life style of tetrahymenas was ancestrally free-living or parasitic. Here, we applied a different statistical strategy, the stochastic character mapping in a combination with the Bayesian approach that accounts also for uncertainty in the inferred phylogeny. The present reconstruction of the ancestral way of life was unambiguous and suggested that the last common ancestor of the subclass Hymenostomatia was parasitic, while that of tetrahymenas was free-living. Consequently, there were at least seven independent shifts back to parasitism/histophagy: one each in the "*paravorax*" and "*australis*" clades, and at a minimum five reversals to parasitism in the "*borealis*" clade (Fig. 8). Interestingly, the BiSSE analyses suggested that the parasitic lineages have slower speciation and net diversification rates than the free-living lineages. In addition, according to the MCMC simulations, the parasitic lineages face a higher risk to become extinct than the free-living lineages (Fig. 9). This contrasts with two other ciliate classes, the Armophorea Lynn, 2004 and the Litostomatea Small and Lynn, 1981, where both

free-living and endosymbiotic lineages occur. Specifically, our previous diversification analyses suggested that the endobiotic armophorean lineages have several times higher speciation and net diversification rates than the free-living armophorean lineages. This is indirectly corroborated also in that there are only about 80 recognized free-living taxa, while almost 200 endosymbiotic forms (Vďačný et al. 2019). A similar picture can be found in litostomateans which include about 300 free-living species (Foissner et al. 1999), while about 1000 endosymbiotic taxa (Cedrola et al. 2020). By contrast, there are about dozen of obligate or facultative parasitic *Tetrahymena* species, while about 60 free-living taxa (Fig. 8). Also this fact along with phylogenetic trees suggests that tetrahymenas were ancestrally very likely free-living and there were multiple independent shifts to parasitism. On the other hand, there was only a single shift to endobiotic life style in case of litostomateans (Vďačný 2018) and two transfers in case of armophoreans (Vďačný et al. 2019). When obligate endobiosis in the digestive tract of both invertebrates and vertebrates was established, then there was a burst of endobiotic armophorean and litostomatean lineages. Obviously, tetrahymenas prefer different evolutionary strategies than armophoreans and litostomateans, and hence their diversification patterns are also different.

Acknowledgments We thank two anonymous reviewers for their valuable comments. We are also grateful to Ján Kočišek, Erik Mravec, Ivan Rúrik, Martin Sečanský, Eva Tirjaková, and Michal Veselický for their help with sampling, and to Ivan Rúrik for his help with some bioinformatics tools.

Funding information This work was supported by the Slovak Research and Development Agency under the contract no. APVV-15-0147, by the Grant Agency of the Ministry of Education, Science, Research and Sport of the Slovak Republic and Slovak Academy of Sciences under the Grant VEGA 1/0041/17, and by the Comenius University in Bratislava under the Grant UK/160/2020.

Compliance with ethical standards

All applicable institutional, national, and international guidelines for the care and use of animals were followed.

Conflict of interest The authors declare that they have no conflict of interest.

References

Antipa GA, Small EB (1971) The occurrence of thigmotrichous ciliated protozoa inhabiting the mantle cavity of unionid molluscs of Illinois. Trans Am Microsc Soc 90:463–472. https://doi.org/10.2307/3225461

Ball IR (1974) A contribution to the phylogeny and biogeography of the freshwater triclads (Platyhelminthes, Turbellaria). In: Riser W, Morse MP (eds) Biology of the Turbellaria. McGraw-Hill, New York, pp 339–401

Batson BS (1983) *Tetrahymena dimorpha* sp. nov. (Hymenostomatida: Tetrahymenidae), a new ciliate parasite of Simuliidae (Diptera) with potential as a model for the study of ciliate morphogenesis. Philos Trans R Soc Lond B 301:345–363. https://doi.org/10.1098/rstb.1983.0027

Batson BS (1985) A paradigm for the study of insect-ciliate relationships: *Tetrahymena sialidos* sp. nov. (Hymenostomatida: Tetrahymenidae), parasite of larval *Sialis lutaria* (Linn.) (Megaloptera: Sialidae). Philos Trans R Soc Lond B 310:123–144. https://doi.org/10.1098/rstb.1985.0102

Blackburn EH, Gall JG (1978) A tandemly repeated sequence at the termini of the extrachromosomal ribosomal RNA genes in *Tetrahymena*. J Mol Biol 120:33–53. https://doi.org/10.1016/0022-2836(78)90294-2

Bollback JP (2006) SIMMAP: stochastic character mapping of discrete traits on phylogenies. BMC Bioinformatics 7:88. https://doi.org/10.1186/1471-2105-7-88

Brooks W (1968) Tetrahymenid ciliates as parasites of the gray garden slug. Hilgardia 39:205–276. https://doi.org/10.3733/hilg.v39n08p205

Brownell JE, Zhou J, Ranalli T, Kobayashi R, Edmondson DG, Roth SY, Allis CD (1996) *Tetrahymena* histone acetyltransferase A: a homolog to yeast Gcn5p linking histone acetylation to gene activation. Cell 84:843–851. https://doi.org/10.1016/s0092-8674(00)81063-6

Brunk CF, Lee LC, Tran AB, Li J (2003) Complete sequence of the mitochondrial genome of *Tetrahymena thermophila* and comparative methods for identifying highly divergent genes. Nucleic Acids Res 31:1673–1682. https://doi.org/10.1093/nar/gkg270

Burger G, Zhu Y, Littlejohn TG, Greenwood SJ, Schnare MN, Lang BF, Gray MW (2000) Complete sequence of the mitochondrial genome of *Tetrahymena pyriformis* and comparison with *Paramecium aurelia* mitochondrial DNA. J Mol Biol 297:365–380. https://doi.org/10.1006/jmbi.2000.3529

Cedrola F, Senra MVX, Rossi MF, Fregulia P, D'Agosto M, Dias RJP (2020) Trichostomatid ciliates (Alveolata, Ciliophora, Trichostomatia) systematics and diversity: past, present and future. Front Microbiol 10:2967. https://doi.org/10.3389/fmicb.2019.02967

Chantangsi C, Lynn DH, Brandl MT, Cole JC, Hetrick N, Ikonomi P (2007) Barcoding ciliates: a comprehensive study of 75 isolates of the genus *Tetrahymena*. Int J Syst Evol Microbiol 57:2412–2425. https://doi.org/10.1099/ijs.0.64865-0

Corliss JO (1960) *Tetrahymena chironomi* sp. nov., a ciliate from midge larvae, and the current status of facultative parasitism in the genus *Tetrahymena*. Parasitology 50:111–153. https://doi.org/10.1017/s0031182000025245

Corliss JO (1969) An up-to-date analysis of the systematics of the ciliate genus *Tetrahymena*. J Protozool 16:6–7. https://doi.org/10.1111/j.1550-7408.1969.tb04358.x

Corliss JO (1970) The comparative systematics of species comprising the hymenostome ciliate genus *Tetrahymena*. J Protozool 17:198–209. https://doi.org/10.1111/j.1550-7408.1970.tb02356.x

Corliss JO (1972) *Tetrahymena* and some thoughts on the evolutionary origin of endoparasitism. Trans Am Microsc Soc 91:566–573. https://doi.org/10.2307/3225485

Corliss JO (1973) History, taxonomy, ecology, and evolution of species of *Tetrahymena*. In: Elliott AM (ed) Biology of *Tetrahymena*. Dowden, Hutchinson & Ross, Stroudsburg, pp 1–55

Dahm AG (1958) Taxonomy and ecology of five species groups in the family Planariidae (Turbellaria Tricladida Paludicola). Nya Litografen, Malmö

Darriba D, Taboada GL, Doallo R, Posada D (2012) jModelTest 2: more models, new heuristics and parallel computing. Nat Methods 9:772. https://doi.org/10.1038/nmeth.2109

Doerder FP (2014) Abandoning sex: multiple origins of asexuality in the ciliate *Tetrahymena*. BMC Evol Biol 14:112. https://doi.org/10.1186/1471-2148-14-112

Doerder FP (2019) Barcodes reveal 48 new species of *Tetrahymena*, *Dexiostoma*, and *Glaucoma*: phylogeny, ecology, and biogeography of new and established species. J Eukaryot Microbiol 66:182–208. https://doi.org/10.1111/jeu.12642

Edqvist J, Burger G, Gray MW (2000) Expression of mitochondrial protein-coding genes in *Tetrahymena pyriformis*. J Mol Biol 297: 381–393. https://doi.org/10.1006/jmbi.2000.3530

FitzJohn RG (2012) Diversitree: comparative phylogenetic analyses of diversification in R. Methods Ecol Evol 3:1084–1092. https://doi.org/10.1111/j.2041-210X.2012.00234.x

Foissner W (2014) An update of 'basic light and scanning electron microscopic methods for taxonomic studies of ciliated protozoa'. Int J Syst Evol Microbiol 64:271–292. https://doi.org/10.1099/ijs.0.057893-0

Foissner W, Berger H, Schaumburg J (1999) Identification and ecology of limnetic plankton ciliates. Informationsberichte des Bayer Landesamtes für Wasserwirtschaft 3(99):1–793

Frankel J (1999) Cell biology of *Tetrahymena thermophila*. Methods Cell Biol 125:27–125

Furgason WH (1940) The significant cytostomal pattern of the "*Glaucoma-Colpidium* group," and a proposed new genus and species, *Tetrahymena geleii*. Arch Protistenkd 94:224–266

Greider CW, Blackburn EH (1985) Identification of a specific telomere terminal transferase activity in *Tetrahymena* extracts. Cell 43:405–413. https://doi.org/10.1016/0092-8674(85)90170-9

Hall TA (1999) BioEdit: a user-friendly biological sequence alignment editor and analysis program for Windows 95/98/NT. Nucleic Acids Symp Ser 41:95–98

International Commission on Zoological Nomenclature (1999) International code of zoological nomenclature, 4th edn. Tipografia La Garangola, Padova

International Commission on Zoological Nomenclature (2012) Amendment of Articles 8, 9, 10, 21 and 78 of the International Code of Zoological Nomenclature to expand and refine methods of publication. Bull Zool Nomencl 69:161–169

Jerome CA, Simon EM, Lynn DH (1996) Description of *Tetrahymena empidokyrea* n.sp., a new species in the *Tetrahymena pyriformis* sibling species complex (Ciliophora, Oligohymenophorea), and an assessment of its phylogenetic position using small-subunit rRNA sequences. Can J Zool 74:1898–1906. https://doi.org/10.1139/z96-214

Johnson MTJ, FitzJohn RG, Smith SD, Rausher MD, Otto SP (2011) Loss of sexual recombination and segregation is associated with increased diversification in evening primroses. Evolution 65:3230–3240. https://doi.org/10.1111/j.1558-5646.2011.01378.x

Kass RE, Raftery AE (1995) Bayes factors. J Am Stat Assoc 90:773–795. https://doi.org/10.1080/01621459.1995.10476572

Kawakatsu M, Oki I, Tamura S, Yamayoshi T (1985) Reexamination of freshwater planarians found in tanks of tropical fishes in Japan, with a description of a new species, *Dugesia austroasiatica* sp. nov. (Turbellaria; Tricladida; Paludicola). Bull Biogeogr Soc Jpn 40:1–19

Kher CP, Doerder FP, Cooper J, Ikonomi P, Achilles-Day U, Küpper FC, Lynn DH (2011) Barcoding *Tetrahymena*: discriminating species and identifying unknowns using the cytochrome c oxidase subunit I (cox-1) barcode. Protist 162:2–13. https://doi.org/10.1016/j.protis.2010.03.004

Kozloff EN (1946) The morphology and systematic position of a holotrichous ciliate parasitizing *Deroceras agreste* (L.). J Morphol 79:445–465. https://doi.org/10.1002/jmor.1050790305

Kumar S, Stecher G, Li M, Knyaz C, Tamura K (2018) MEGA X: molecular evolutionary genetics analysis across computing platforms. Mol Biol Evol 35:1547–1549. https://doi.org/10.1093/molbev/msy096

Lwoff A (1923) Sur la nutrition des infusoires. C R Acad Sci 176:928–930

Lynn DH (2008) The ciliated protozoa. Characterization, classification and guide to the literature. Springer, Dordrecht

Lynn DH, Doerder FP (2012) The life and times of *Tetrahymena*. Methods Cell Biol 109:9–27. https://doi.org/10.1016/B978-0-12-385967-9.00002-5

Lynn DH, Doerder FP, Gillis PL, Prosser PS (2018) *Tetrahymena glochidiophila* n. sp., a new species of *Tetrahymena* (Ciliophora) that causes mortality to glochidia larvae of freshwater mussels (Bivalvia). Dis Aquat Org 127:125–136. https://doi.org/10.3354/dao03188

Lynn DH, Molloy D, LeBrun R (1981) *Tetrahymena rotunda* n. sp. (Hymenostomatida: Tetrahymenidae), a ciliate parasite of the hemolymph of *Simulium* (Diptera: Simuliidae). Trans Am Microsc Soc 100:134–141. https://doi.org/10.2307/3225796

Lynn DH, Strüder-Kypke MC (2006) Species of *Tetrahymena* identical by small subunit rRNA gene sequences are discriminated by mitochondrial cytochrome c oxidase I gene sequences. J Eukaryot Microbiol 53:385–387. https://doi.org/10.1111/j.1550-7408.2006.00116.x

MacColl E, Therkelsen MD, Sherpa T, Ellerbrock H, Johnston LA, Jariwala RH, Chang WS, Gurtowski J, Schatz MC, Mozammal Hossain M, Cassidy-Hanley DM, Clark TG, Chang WJ (2015) Molecular genetic diversity and characterization of conjugation genes in the fish parasite *Ichthyophthirius multifiliis*. Mol Phylogenet Evol 86:1–7. https://doi.org/10.1016/j.ympev.2015.02.017

Maddison WP, Midford PE, Otto SP (2007) Estimating a binary character's effect on speciation and extinction. Syst Biol 56:701–710. https://doi.org/10.1080/10635150701607033

Medlin L, Elwood HJ, Stickel S, Sogin ML (1988) The characterization of enzymatically amplified eukaryotic 16S-like rRNA coding regions. Gene 71:491–499. https://doi.org/10.1016/0378-1119(88)90066-2

Miller MA, Pfeiffer W, Schwartz T (2010) Creating the CIPRES Science Gateway for inference of large phylogenetic trees. In: Proceedings of the Gateway Computing Environments Workshop (GCE). Piscataway, N.J., New Orleans, Louisiana, pp 1–8. https://doi.org/10.1109/GCE.2010.5676129

Moradian MM, Beglaryan D, Skozylas JM, Kerikorian V (2007) Complete mitochondrial genome sequence of three *Tetrahymena* species reveals mutation hot spots and accelerated nonsynonymous substitutions in Ymf genes. PLoS One 2:e650. https://doi.org/10.1371/journal.pone.0000650

Nanney DL, McCoy JW (1976) Characterization of the species of the *Tetrahymena pyriformis* complex. Trans Am Microsc Soc 95:664–682. https://doi.org/10.2307/3225391

Nanney DL, Park C, Preparata R, Simon EM (1998) Comparison of sequence differences in a variable 23S rRNA domain among sets of cryptic species of ciliated protozoa. J Eukaryot Microbiol 45:91–100. https://doi.org/10.1111/j.1550-7408.1998.tb05075.x

Nekuie Fard A, Motalebi AA, Jalali Jafari B, Aghazadeh Meshgi M, Azadikhah D, Afsharnasab M (2011) Survey on fungal, parasites and epibionts infestation on the *Astacus leptodactylus* (Eschscholtz, 1823), in Aras reservoir West Azarbaijan, Iran. Iran J Fish Sci 10:266–275

Nguyen LT, Schmidt HA, von Haeseler A, Minh BQ (2015) IQ-TREE: a fast and effective stochastic algorithm for estimating maximum-likelihood phylogenies. Mol Biol Evol 32:268–274. https://doi.org/10.1093/molbev/msu300

Pitsch G, Adamec L, Dirren S, Nitsche F, Šimek K, Sirová D, Posch T (2017) The green *Tetrahymena utricolariae* n. sp. (Ciliophora, Oligohymenophorea) with its endosymbiotic algae (*Micractinium*

sp.), living in traps of a carnivorous aquatic plant. J Eukaryot Microbiol 64:322–335. https://doi.org/10.1111/jeu.12369

Quintela-Alonso P, Nitsche F, Wylezich C, Arndt H, Foissner W (2013) A new *Tetrahymena* (Ciliophora, Oligohymenophorea) from groundwater of Cape Town, South Africa. J Eukaryot Microbiol 60:235–246. https://doi.org/10.1111/jeu.12021

Rataj M, Vďačný P (2018) Dawn of astome ciliates in light of morphology and time-calibrated phylogeny of *Haptophrya planariarum*, an obligate endosymbiont of freshwater turbellarians. Eur J Protistol 64:54–71. https://doi.org/10.1016/j.ejop.2018.03.004

Rataj M, Vďačný P (2019) Living morphology and molecular phylogeny of oligohymenophorean ciliates associated with freshwater turbellarians. Dis Aquat Org 134:147–166. https://doi.org/10.3354/dao03366

Revell LJ (2012) Phytools: an R package for phylogenetic comparative biology (and other things). Methods Ecol Evol 3:217–223. https://doi.org/10.1111/j.2041-210X.2011.00169.x

Reynoldson TB, Bellamy LS (1973) Interspecific competition in lake-dwelling triclads. A laboratory study. Oikos 24:301–313

Ronquist F, Teslenko M, van der Mark P, Ayres DL, Darling A, Höhna S, Larget B, Liu L, Suchard MA, Huelsenbeck JP (2012) MrBayes 3.2: efficient Bayesian phylogenetic inference and model choice across a large model space. Syst Biol 61:539–542. https://doi.org/10.1093/sysbio/sys029

Silvestro D, Schnitzler J, Zizka G (2011) A Bayesian framework to estimate diversification rates and their variation through time and space. BMC Evol Biol 11:311. https://doi.org/10.1186/1471-2148-11-311

Strüder-Kypke MC, Wright ADG, Jerome CA, Lynn DH (2001) Parallel evolution of histophagy in ciliates of the genus *Tetrahymena*. BMC Evol Biol 1:5. https://doi.org/10.1186/1471-2148-1-5

van Hoek AHAM, Akhmanova AS, Huynen MA, Hackstein JHP (2000) A mitochondrial ancestry of the hydrogenosomes of *Nyctotherus ovalis*. Mol Biol Evol 17:202–206. https://doi.org/10.1093/oxfordjournals.molbev.a026234

Vďačný P (2018) Evolutionary associations of endosymbiotic ciliates shed light on the timing of the marsupial-placental split. Mol Biol Evol 35:1757–1769. https://doi.org/10.1093/molbev/msy071

Vďačný P, Bourland WA, Orsi W, Epstein SS, Foissner W (2011) Phylogeny and classification of the Litostomatea (Protista, Ciliophora), with emphasis on free-living taxa and the 18S rRNA gene. Mol Phylogenet Evol 59:510–522. https://doi.org/10.1016/j.ympev.2011.02.016

Vďačný P, Rajter Ľ, Stoeck T, Foissner W (2019) A proposed timescale for the evolution of armophorean ciliates: clevelandellids diversify more rapidly than metopids. J Eukaryot Microbiol 66:167–181. https://doi.org/10.1111/jeu.12641

Warren A, Patterson DJ, Dunthorn M, Clamp JC, Achilles-Day UEM, Aescht E, al-Farraj SA, al-Quraishy S, al-Rasheid K, Carr M, Day JG, Dellinger M, el-Serehy HA, Fan Y, Gao F, Gao S, Gong J, Gupta R, Hu X, Kamra K, Langlois G, Lin X, Lipscomb D, Lobban CS, Luporini P, Lynn DH, Ma H, Macek M, Mackenzie-Dodds J, Makhija S, Mansergh RI, Martín-Cereceda M, McMiller N, Montagnes DJS, Nikolaeva S, Ong'ondo G, Pérez-Uz B, Purushothaman J, Quintela-Alonso P, Rotterová J, Santoferrara L, Shao C, Shen Z, Shi X, Song W, Stoeck T, la Terza A, Vallesi A, Wang M, Weisse T, Wiackowski K, Wu L, Xu K, Yi Z, Zufall R, Agatha S (2017) Beyond the 'code': a guide to the description and documentation of biodiversity in ciliated protists (Alveolata, Ciliophora). J Eukaryot Microbiol 64:539–544. https://doi.org/10.1111/jeu.12391

Wright JF (1969) The ecology of stream-dwelling triclads. Dissertation, University of Wales

Wright JF (1981) *Tetrahymena pyriformis* (Ehrenberg) and *T. corlissi* Thompson parasitic in stream-dwelling triclads (Platyhelminthes: Turbellaria). J Parasitol 67:131–133. https://doi.org/10.2307/3280799

Yao MC, Blackburn EH, Gall JG (1981) Tandemly repeated C-C-C-C-A-A hexanucleotide of *Tetrahymena* rDNA is present elsewhere in the genome and may be related to the alteration of the somatic genome. J Cell Biol 90:515–520. https://doi.org/10.1083/jcb.90.2.515

Yao MC, Yao CH (1981) Repeated hexanucleotide C-C-C-C-A-A is present near free ends of macronuclear DNA of *Tetrahymena*. Proc Natl Acad Sci U S A 78:7436–7439. https://doi.org/10.1073/pnas.78.12.7436

Zahid MT, Shakoori FR, Zulifqar S, Jahan N, Shakoori AR (2014) A new ciliate species, *Tetrahymena farahensis*, isolated from the industrial wastewater and its phylogenetic relationship with other members of the genus *Tetrahymena*. Pakistan J Zool 46:1433–1445